Dynamics of Gene Expression Responses for Ion Transport Proteins and Aquaporins in the Gill of a Euryhaline Pupfish during Freshwater and High-Salinity Acclimation

Sean C. Lema[1],*
Paul G. Carvalho[1],†
Jennifer N. Egelston[1]
John T. Kelly[2],‡
Stephen D. McCormick[3]

[1]Biological Sciences Department, Center for Coastal Marine Sciences, California Polytechnic State University, San Luis Obispo, California 93407; [2]Department of Biology and Environmental Science, University of New Haven, West Haven, Connecticut 06516; [3]US Geological Survey, Leetown Science Center, Conte Anadromous Fish Research Laboratory, Turners Falls, Massachusetts 01376; and Department of Biology, University of Massachusetts, Amherst, Massachusetts 01003

ABSTRACT

Pupfishes (genus *Cyprinodon*) evolved some of the broadest salinity tolerances of teleost fishes, with some taxa surviving in conditions from freshwater to nearly 160 ppt. In this study, we examined transcriptional dynamics of ion transporters and aquaporins in the gill of the desert Amargosa pupfish (*Cyprinodon nevadensis amargosae*) during rapid salinity change. Pupfish acclimated to 7.5 ppt were exposed to freshwater (0.3 ppt), seawater (35 ppt), or hypersaline (55 ppt) conditions over 4 h and sampled at these salinities over 14 d. Plasma osmolality and Cl^- concentration became elevated 8 h after the start of exposure to 35 or 55 ppt but returned to baseline levels after 14 d. Osmolality recovery was paralleled by increased gill Na^+/K^+-ATPase activity and higher relative levels of messenger RNAs (mRNAs) encoding cystic fibrosis transmembrane conductance regulator (*cftr*) and $Na^+/K^+/2Cl^-$ cotransporter-1 (*nkcc1*). Transcripts encoding one Na^+-HCO_3^- cotransporter-1 isoform (*nbce1.1*) also increased in the gills at higher salinities, while a second isoform (*nbce1.2*) increased expression in freshwater. Pupfish in freshwater also had lower osmolality and elevated gill mRNAs for Na^+/H^+ exchanger isoform-2a (*nhe2a*) and V-type H^+-ATPase within 8 h, followed by increases in Na^+/H^+ exchanger-3 (*nhe3*), carbonic anhydrase 2 (*ca2*), and aquaporin-3 (*aqp3*) within 1 d. Gill mRNAs for Na^+/Cl^- cotransporter-2 (*ncc2*) also were elevated 14 d after exposure to 0.3 ppt. These results offer insights into how coordinated transcriptional responses for ion transporters in the gill facilitate reestablishment of osmotic homeostasis after changes in environmental salinity and provide evidence that the teleost gill expresses two Na^+-HCO_3^- cotransporter-1 isoforms with different roles in freshwater and seawater acclimation.

Introduction

The ability to maintain plasma ionic and osmotic homeostasis across varying environmental salinities has evolved in only 3%–5% of extant fishes (Edwards and Marshall 2013; Schultz and McCormick 2013). Typically, these euryhaline fishes occupy habitats such as coastal estuaries characterized by fluctuating salinities or have evolved a diadromous life history where they move between freshwater (FW) and marine environments. In the arid deserts of southwestern North America, however, nearly 40 species of euryhaline pupfishes (genus *Cyprinodon*) occupy isolated aquatic environments including groundwater-fed FW springs, saline marshes, and small, intermittent desert streams (e.g., LaBounty and Deacon 1972; Soltz and Naiman 1978). Even though many of these desert species no longer experience large salinity fluctuations in their habitats, desert pupfishes—like their congeners inhabiting estuaries and other coastal areas of the western Atlantic Ocean and Caribbean Sea—retain extraordinary abilities for tolerating osmotic stress (e.g., Nordlie 2006; Whitehead 2010; Ghedotti and Davis 2013). Pupfishes have been found in hypersaline environments over 160 ppt, and experimental studies have documented that some taxa can maintain osmotic balance under conditions from ~0 mOsm (~0 ppt) to 3,000 mOsm (105 ppt; Simpson and Gunter 1956; Barlow 1958; Renfro and Hill 1971; Naiman et al. 1976; Gerking and Lee 1980; Gilmore et al. 1982; Nordlie 1985; Jordan et al. 1993).

The physiological capacity of pupfishes and other cyprinodontoid fishes to acclimate to such a wide range of salinities

*Corresponding author; email: slema@calpoly.edu.
†Present address: Department of Fisheries, Animal and Veterinary Sciences, University of Rhode Island, Kingston, Rhode Island 02881.
‡Present address: California Department of Fish and Wildlife, Fisheries Branch, 830 S Street, Sacramento, California 95811.

involves integrated mechanisms of ionoregulation and osmo-regulation across several tissues, including the gills, intestine, and kidneys (Laverty and Skadhauge 2012; Edwards and Marshall 2013). In teleost fishes, the gill is considered the dominant tissue for ionoregulation during rapid shifts to hypo- or hyper-osmotic conditions (Evans et al. 2005; Hwang et al. 2011; Edwards and Marshall 2013), and the maintenance of osmotic homeostasis in desert pupfishes likely involves coordinated adjustments in ion and water transport across this tissue (e.g., Stuenkel and Hillyard 1980, 1981). During acclimation of a related cyprinodontoid fish, the euryhaline mummichog (*Fundulus heteroclitus*), to seawater (SW), epithelial Na^+/K^+ ATPase (NKA) activity increases in ion-ocytes (also called "mitochondrion-rich" cells) of the gills within minutes (Towle et al. 1977; Mancera and McCormick 2000). Elevated NKA activity creates a Na^+ electrochemical gradient, which drives Cl^- transport from the blood into the ionocyte, via $Na^+/K^+/2Cl^-$ cotransporter-1 (Nkcc1) on the basolateral membrane of the ionocyte (Flemmer et al. 2010), and subsequently Cl^- from the ionocyte to the external SW environment by the cystic fibrosis transmembrane conductance regulator (Cftr) Cl^- channel on the apical ionocyte membrane (Marshall et al. 1999, 2002).

During acclimation of mummichog to FW, passive ion loss is countered by Na^+ and Cl^- uptake by the gill (Patrick et al. 1997; Patrick and Wood 1999), although ion uptake via the intestines also is critical to maintain ionic balance under very low environmental salinities (Marshall et al. 1997). Na^+ uptake by the teleost gill often occurs through the action of a V-type H^+-ATPase enzyme that generates an electrochemical gradient for Na^+ to enter the ionocyte via an epithelial Na^+ channel (Evans et al. 2005). However, unlike in rainbow trout (*Oncorhynchus mykiss*), where a V-type H^+-ATPase enzyme in the apical membrane facilitates ion uptake (Lin et al. 1994; Evan et al. 2005), the V-type H^+-ATPase in the ionocytes of mummichog is expressed in the basolateral membrane (Katoh et al. 2003) and may not be involved directly in ion uptake. Instead, Na^+ influx in FW may be mediated in part by gill Na^+/H^+ exchangers (Edwards et al. 2005; Scott et al. 2005). Evidence supporting this idea comes in part from Scott and co-workers (2005), who observed increases in gill Na^+/H^+ exchanger 2 (Nhe2) messenger RNA (mRNA) expression, as well as transcripts encoding the carbonic anhydrase 2 (Ca2) enzyme critical to acid-base balance, after transfer of mummichog from 10 ppt to FW conditions. Recent evidence from other fishes has also pointed to a Na^+/Cl^- cotransporter (Ncc) mediating Na^+ and Cl^- uptake across the gill in FW (Hiroi et al. 2008; Wang et al. 2009).

The electrogenic Na^+-HCO_3^- cotransporter-1 (NBCe1) has also been implicated in gill epithelial Na^+ transport as well as acid-base regulation in teleosts (Parks et al. 2007). Cl^- and Na^+ uptake across ionocytes is directly linked to the secretion of HCO_3^- and H^+ (Goss and Wood 1990; Patrick et al. 1997; Perry et al. 2003), since changes in ionocyte pH influence ion uptake. Parks and colleagues (2007) proposed that NBCe1 might work in concert with the Ca2 enzyme to drive Na^+ efflux in fish under hypoosmotic conditions. Mammalian NBCe1 binds the Ca2 enzyme on its C terminal (Gross et al. 2002; Romero et al. 2004), and production of HCO_3^- by Ca2 enzymatic activity in ionocytes may occur in sufficiently close proximity to NBCe1 that NBCe1 drives

Na^+ transport across the basolateral membrane even in the face of an unfavorable Na^+ electrochemical gradient across the ion-ocyte membrane as a whole (Parks et al. 2007). Teleost fishes, however, have evolved at least two NBCe1 transporters (Lee et al. 2011; Chang et al. 2012), and despite the possibility of an important role for NBCe1 in maintaining acid-base and osmotic homeostasis in teleost fishes, no study—to our knowledge—had yet compared the expressional responses or functional roles of these two teleost NBCe1 isoforms.

In this study, we examined gene transcription changes for ion transporters and aquaporins in the gill epithelium of the desert Amargosa pupfish *Cyprinodon nevadensis amargosae* during acclimation to rapidly changing salinity conditions. The Amargosa pupfish inhabits the Amargosa River, located in the Death Valley region of California and Nevada, and is part of a clade of pupfishes that diversified from a common ancestor into nine taxa within this geographic region (Miller 1950; Soltz and Naiman 1978). Death Valley pupfishes occupy remote streams, springs, and marshes that vary in salinity from FW (0.4 ppt) to hypersaline (>70 ppt) conditions (Naiman et al. 1976; Soltz and Naiman 1978). The Amargosa River experiences rapid shifts in salinity (range: 0.2–12.7 ppt) as the habitat alternates between desiccation under the extreme heat of Death Valley's summer and flooding that can occur after rainfall events (e.g., Tanko and Glancy 2001). In our study, adult Amargosa pupfish acclimated to a brackish salinity (7.5 ppt) were transferred to FW (0.3 ppt), SW (35 ppt), or hypersaline (55 ppt) conditions over a 4-h period. We then quantified the effects of these salinity changes on plasma osmo-lality, Cl^- concentrations, NKA activity in the gill epithelium, and gill transcript abundance encoding the two teleost isoforms of NBCe1, *nbce1.1* and *nbce1.2*, as well as several other critical ion transporters. We also quantified relative mRNA levels of aquaporin-1 (*aqp1*) and aquaporin-3 (*aqp3*) in the gill epithelium as well as the relative transcript abundance for osmotic transcription factor-1 (*ostf1*), an osmosensor implicated in detecting and responding to osmolality changes in order to regulate appropriate transcriptional responses in cells to maintain ion and water homeostasis (e.g., Fiol and Kültz 2005, 2007; Fiol et al. 2006). Our data document the temporal dynamics of gene expression in the gill during acclimation to FW or high-salinity environments and provide evidence that the teleost gill may express two NBCe1 isoforms with different patterns of transcriptional regulation suggestive of divergent roles in FW and SW acclimation.

Material and Methods

Experimental Animals

Adult Amargosa pupfish (*Cyprinodon nevadensis amargosae*) were collected from the Amargosa River (35°51.275′N, 116° 13.833′W) on November 18, 2012. Salinity of the Amargosa River on the day of collection was 7.5 ppt (YSI 85 field meter, YSI, Yellow Springs, OH). Fish were transferred to holding facilities at California Polytechnic State University and maintained in 208-L closed-system tanks, under conditions of a 14L : 10D photoperiod and 24°–25°C, containing 7.5-ppt-salinity water made with In-

stant Ocean salt (Unified Pet Group, Blacksburg, VA) and de-ioinized water. Fish were fed a 1:1 mixture of commercial spi-rulina flake (Aquatic Eco-Systems, Apopka, FL) and brine shrimp flake (San Francisco Bay Brand, Newark, CA) feeds ad lib. daily. All procedures were approved by the Animal Care and Use Com-mittee of California Polytechnic State University (protocol 1507).

Isolation and Sequencing of Partial Complementary DNAs

Total RNA was extracted from gill and digestive tract tissues of an adult male Amargosa pupfish (43.1 mm standard length [SL]; 2.64 g body mass) using TriReagent (Molecular Research Center, Cincinnati), with bromochloropropane as the phase separation reagent. The extraction RNA samples were DNase I treated (TURBO DNA-Free Kit, Ambion), quantified by spec-trophotometry (260:280 ratios > 2.00; NanoPhotometer P300, Implen, Westlake Village, CA), and examined on a 0.8% agarose gel for RNA quality.

First-strand complementary DNA (cDNA) was generated in 20-μL reverse-transcription reactions by incubating 5 μg of total RNA template (4.0 μL) with 1.0 μL of random primers (random hexadeoxynucleotides; Promega, Madison, WI) at 70°C for 10 min. The above mixture was then combined with 3.0 μL of MgCl$_2$ (25 mM), 1.0 μL of deoxynucleotide triphos-phates (dNTPs; 100 mM, Promega), 0.25 μL of recombinant RNasin ribonuclease inhibitor (20 U/μL, Promega), 4.0 μL of 5× reaction buffer, 0.5 μL of GoScript reverse transcriptase, and 6.25 μL of nuclease-free H$_2$O, as per the protocol of the GoScript Reverse Transcription System (Promega). RNA was reverse-transcribed under a thermal profile of 25°C for 5 min and 42°C for 1 h, followed by 70°C for 15 min to inactivate the reverse transcriptase enzyme (T100 thermal cycler, Bio-Rad Laboratories, Hercules, CA).

Nested sets of degenerate primers (Integrated DNA Tech-nologies, Coralville, IA) were designed to consensus regions of previously published cDNA sequences from other teleost fishes. Descriptions of the cDNA sequences used to design these prim-ers are provided in the appendix, and nucleotide sequences for these primers are presented in table A1.

Polymerase chain reactions (PCRs; 50 μL) using these nested degenerate primers or gene-specific primers for *v-ATPaseβ* were run under the following reaction conditions: 94°C for 2 min; 35 cycles of 94°C for 30 s, 48°–54°C for 30 s, and 72°C for 1–2.5 min; and then 72°C for 2–4 min. Annealing temperatures and extension times varied in accordance with the melting tem-peratures and expected product sizes for each reaction. All cDNAs were amplified from RNA isolated from gill except *nkcc2* and *ca*, which were amplified from RNA isolated from intestine. PCR products were examined on 1.2% ethidium bromide (EtBr) gels, and then a second round of nested PCRs was run with the following thermal profile: 94°C for 2 min; 30 cycles of 94°C for 30 s, 50°–55°C for 30 s, and 72°C for 1–2.5 min; and then 72°C for 2–4 min. After electrophoresis on 1.2% EtBr gels, any PCR products with single bands of expected product size were cleaned (QIAquick PCR Purification Kit, Qiagen), quantified by spectro-photometry (NanoPhotometer P300, Implen), and sequenced with

Sanger sequencing methods (Macrogen USA, Rockville, MD). Re-sulting nucleotide sequences for the same transcript were assembled with Sequencher 5.0.1 software (GeneCodes, Ann Arbor, MI) and compared for identity against previously published sequences in teleost fishes with the National Center for Biotechnology Infor-mation BLAST program (http://blast.ncbi.nlm.nih.gov/). For some of these transcripts, additional confirmation of transcript identity was performed by constructing a phylogeny using the deduced amino acid sequences from the partial cDNAs and homologous transcripts from other vertebrates available on GenBank.

Acute Salinity Exposure Challenge

Fish collected on November 18, 2012, were maintained at 7.5-ppt salinity in 208-L tanks in captivity for 5 mo before being moved to smaller (38-L) experimental treatment tanks at 7.5-ppt salinity. Six fish (3 males, 3 females) were placed in each 38-L tank, and a total of eight replicate tanks were used for each treatment. Fish were maintained in these treatment tanks for 14 d before sa-linity changes. Salinity conditions were created by the addition of Instant Ocean salts to deionized water. The ionic composition of Instant Ocean salts is provided by Atkinson and Bingman (1997). Salinities in each tank were recorded daily (YSI 85), and tank temperatures (mean ± SD: 26.6° ± 1.2°C; no differences among treatment groups) were recorded every 30 min (HOBO U12 Ex-ternal Data Loggers, Onset, Bourne, MA). Fish were fed ad lib. a 1:1 mixture of spirulina and brine shrimp flake food throughout the experiment.

In the hour immediately before the salinity change began, one fish from each of the eight 38-L tanks ($n = 8$) was netted and euthanized in tricaine methansulfonate (MS222, at 300 mg/L, followed by cervical dislocation), to provide an initial ("base-line") sample of fish acclimated to 7.5 ppt before the salinity changes. Euthanized fish were measured and weighed, and blood was collected into heparinized capillary tubes after the caudal peduncle was severed. Plasma was collected by centri-fugation of the blood at 3,000 *g* for 10 min at 4°C and then stored at −80°C. The first, second, and third gill arches on the right side of each fish were dissected and immediately frozen in liquid N$_2$ for gene expression analyses. Filament tissue from the first, second, and third gill arches on the left side of each fish was isolated and preserved in a sucrose-Na$_2$EDTA-imidazole (SEI) buffer for subsequent quantification of NKA activity.

Over a 4-h period, the salinity conditions in each tank were then decreased, increased, or maintained constant (7.5 ppt, control) to create the following treatments: 0.3 ppt (FW: 18 mOsm kg^{-1}, pH 7.66), 35 ppt (SW: 1,060 mOsm kg^{-1}, pH 8.19), 55 ppt (hypersaline: 1,730 mOsm kg^{-1}, pH 8.27), and 7.5 ppt (control: 216 mOsm kg^{-1}, pH 7.68). Eight replicate tanks were used for each treatment group. Salinity conditions in each tank were re-duced by gradual replacement of the 7.5 ppt water with pure de-ionized water of the same temperature or increased by the addition of Instant Ocean salts to the sump tank associated with each tank's biological filter system. This method for salinity alteration resulted in experimental fish experiencing a change in environmental ion concentration without any need for netting and transferring fish

or any other disruption (e.g., changes in water flow, temperature, pump sounds) that could have induced a physiological stress response beyond that from the change in salinity. The control treatment (7.5 ppt) also went through a water change with same-temperature 7.5-ppt water over the comparable 4-h period to control for any unintended effects of transitioning water chemical composition (e.g., amino acids, fish waste products) beyond salinity condition. Two unintentional mortalities occurred among pupfish in the 55-ppt treatment within 4 d of the salinity change.

One fish was then sampled from each of the eight replicate tanks at time periods of 8 h, 24 h, 96 h (4 d), and 14 d after the change in salinity began. The first sampling, at a time of 8 h, therefore represents 8 h after the beginning of the change in environmental salinity, which corresponds to 4 h after the salinity change was completed. At each sampling time, fish were euthanized with MS222 and then measured and weighed (females: 34.8 ± 0.5 mm SL, 1.41 ± 0.06 g mass; males: 39.9 ± 0.6 mm SL, 2.37 ± 0.10 g mass; mean ± SEM). Blood was collected in heparinized capillary tubes from the caudal peduncle, transferred to heparinized microcentrifuge tubes, and centrifuged at 3,000 g for 10 min at 4°C. The resulting plasma was collected and stored at −80°C. Gill filaments for RNA extraction and NKA activity were collected as described above and stored at −80°C.

Plasma Osmolality and Chloride Ion Measurement

Plasma osmolality was quantified from a 5-μL volume for each fish with a Wescor 5500 Vapor Pressure Osmometer (Wescor, Logan, UT). Water samples from each of the recirculating systems were also collected, and the osmolality was determined as above. Water samples were measured in triplicate, and, when possible, plasma samples were run in duplicate. Sample sizes for plasma samples were $n = 7$–8 fish per treatment and sampling time. Osmolality measurements had a coefficient of variation of 3.0% for duplicate assays for each sample.

Chloride ion concentration was measured in 6-μL volumes of plasma via coulometric titration using a SAT-500 Salt/Chloride Analyzer (DKK-TOA, Tokyo). Cl^- ion standards ranged from 0.10 to 0.20 mol L^{-1}. Because of the limited volume of plasma obtained from individual pupfish, sample sizes for plasma chloride were reduced to $n = 2$–5 fish per treatment and sampling time.

Gill NKA Activity

Gill NKA activity was determined with a temperature-regulated microplate protocol described previously by McCormick (1993). Briefly, gill filament tissue was homogenized in SEI buffer (100 μL) and pelleted by centrifugation, and the supernatant (10 μL) was mixed with another 50 μL of SEI buffer containing 0.3% Na^+ deoxycholic acid. Ouabain-sensitive NKA activity was quantified as the production of ADP and NADH oxidation in the presence and absence of 0.5 mM ouabain, an NKA inhibitor. All samples were quantified in duplicate in 96-well plates and measured at 340 nm for 10 min at 25°C with a THERMOmax microplate reader (Molecular Devices, Menlo Park, CA). NKA activity was deter-mined as the difference between the NADH decay slopes with and without ouabain and then normalized to the sample's respective total protein concentration. Protein concentrations for each homogenate were measured with a Pierce bicinchoninic acid protein assay.

Quantitative Real-Time Reverse-Transcription PCR (qRT-PCR)

Total RNA was extracted from gill tissues with Tri-Reagent as described above. The resulting RNA was DNase I treated (TURBO DNA-Free Kit) and quantified spectrophotometrically (P300 NanoPhotometer; Implen; 260 : 280 ratios > 1.96). Total RNA was then reverse-transcribed in 32-μL reaction volumes containing 16 μL of RNA (65 ng/μL), 1.6 μL of dNTPs (Promega), 1.6 μL of random primers (500 μg/mL; Promega), 0.125 μL of recombinant RNasin ribonuclease inhibitor (40 u/μL; Promega), 0.275 μL of nuclease-free H_2O, 6.4 μL of 5 × buffer, 4.8 μL of $MgCl_2$, and 1.2 μL of GoScript reverse transcriptase (Promega). Reverse-transcription reactions were run under a thermal profile of 25°C for 5 min and 42°C for 1 h, followed by 70°C for 15 min to inactivate the reverse transcriptase.

Primers for SYBR green quantitative real-time PCR assays were designed to protein coding regions of the partial cDNAs for each gene (table A2). Primers were also designed partial cDNAs encoding ribosomal protein L8 (*rpl8*, KJ719257; Lema et al. 2015) and elongation factor-1α (*ef1α*, EU906930; Lema 2010) from Amargosa pupfish for use as internal control genes. All primers were synthesized by Integrated DNA Technologies. Specificity of these SYBR green primer sets was confirmed by Sanger sequencing of PCR products.

Quantitative real-time PCRs were conducted in 16-μL reactions. Each reaction contained 4.5 μL of nuclease-free water (Sigma, St. Louis), 8 μL of iTaq Universal SYBR green Supermix (Bio-Rad), 1 μL each of forward and reverse primers (5 μM), and 1.5 μL of reverse-transcribed cDNA template. The PCR thermal profile for each reaction was 50°C for 2 min, 95°C for 10 min, and 42 cycles of 95°C for 15 s and 59°C for 1 min, and all assays were run on a 7300 Real-Time PCR System (Applied Biosystems). DNA contamination was assessed for each gene by analysis of RNA samples that were not reverse transcribed, and each quantitative PCR (qPCR) run included two samples without cDNA template to further control for contamination. For each gene, a standard curve was made from a pool of RNA from samples representing all treatments and sexes. This pooled sample was serially diluted, and each standard concentration was assayed in triplicate. Correlation coefficients (r^2) for the standard curves were always greater than 0.965. Melt curve analyses were also performed to confirm amplification of a single product and the absence of primer dimers during each qPCR run. PCR efficiencies for each gene were calculated with the equation: efficiency (%) = $(10^{-1/slope} - 1) \times 100$; mean efficiencies are provided in table A2. For each gene, relative mRNA levels were calculated with the standard curve and normalized to the geometric mean of *rpl8* and *ef1α* mRNA expression, which did not vary among treatments. Abundance values of each gene of interest

were then expressed as a relative level by dividing the resulting values by the mean value of the control treatment group.

Statistical Analyses

Plasma osmolality data were square root transformed to equalize variances before analysis. Osmolality values were first compared at the baseline time period, with a one-factor ANOVA, and then compared, also with a one-factor ANOVA model, within the 7.5-ppt group across all time points to evaluate whether plasma osmolality in the control varied over sampling times. Treatment and time effects on plasma osmolality were then determined with a two-factor ANOVA model with salinity treatment, sampling time, and treatment × time interaction as factors, followed by Tukey-Kramer HSD tests for multiple pairwise comparisons within each sampling time.

Plasma Cl⁻ concentrations were examined with a two-factor ANOVA with salinity treatment, sampling time, and treatment × time interaction. No pairwise post hoc statistical tests were performed on these data, however, given the reduced level of replication ($n = 2–5$ fish) at each treatment–time point combination.

Gill NKA activity data were analyzed with two-factor ANOVA models with salinity treatment, sampling time, and treatment × time interaction and then Tukey-Kramer HSD tests for multiple pairwise comparisons within each sampling time. Gill NKA activity was also compared at the baseline time period among treatment groups with a one-factor ANOVA to test for differences along treatment groups in the baseline 7.5-ppt condition as well as with a one-factor ANOVA model to test for changes in NKA activity across all sampling time points within the 7.5-ppt control group.

In cases where gene expression data failed to conform to the assumptions of normality or equal variances (Levene's tests), data were square root transformed before statistical analyses. Relative levels of mRNAs encoding each gene, as well as the geometric mean of *rpl8* and *ef1α*, were first compared among treatment groups at the baseline ($t = 0$) sampling period with a one-factor ANOVA to determine whether treatment groups varied before alteration of environmental salinity. Results from that comparison showed that baseline values of all mRNAs were similar among treatment groups; only baseline values of *nkcc2* transcripts approached a significant difference ($F_{3,28} = 2.638$, $P = 0.069$), even though gill *nkcc2* was not observed to be affected by a change in salinity (see "Results" below). Control group (7.5-ppt) samples at each time point were then compared by means of a one-factor ANOVA model to evaluate whether relative mRNA levels varied in the control treatment over time. These comparisons confirmed that the relative abundance of all measured transcripts in the gill did not significantly vary in control (7.5-ppt) fish over the 14-d duration of the experiment (range: $P = 0.343–0.984$). Relative transcript abundance levels for each gene were then examined with two-factor ANOVA models with salinity treatment, sampling time, and treatment × time interaction as factors, followed by Tukey-Kramer HSD tests for multiple pairwise comparisons within a sampling time.

All data are shown as mean ± SEM values. All statistical analyses were two-tailed, used $\alpha = 0.05$, and were performed in JMP Pro 12.2.0 software (SAS Institute, Cary, NC).

Results

Plasma Osmolality and Cl⁻ Concentration

Plasma osmolality of pupfish sampled at the baseline measurement time from 7.5-ppt conditions averaged 366 ± 13.5 mOsm kg⁻¹ (mean ± SD) and was similar across all treatment groups ($F_{3,28} = 0.092$, $P = 0.9638$). Significant changes in plasma osmolality were observed in fish exposed to differing salinities, beginning 8 h after salinity alteration (treatment × time interaction: $F_{12,137} = 22.445$, $P < 0.0001$; fig. 1A). Pupfish transferred to 35- or 55-ppt conditions experienced rapid increases in plasma osmolality and reached maximal concentrations of ~490 mOsm kg⁻¹ for 35-ppt pupfish and over 640 mOsm kg⁻¹ for 55-ppt pupfish at 1 d after salinity transfer (compared to the mean osmolality concentration of ~360 mOsm kg⁻¹ observed in 7.5-ppt pupfish). By 14 d, plasma osmolality of pupfish in these 35- and 55-ppt conditions had returned to ~390 mOsm kg⁻¹ and was no longer statistically different from the osmolality of fish maintained at 7.5 ppt. Pupfish transferred to 0.3-ppt conditions experienced a decline in plasma osmolality, to 310 mOsm kg⁻¹, at 1 d after salinity transfer and likewise recovered to a mean concentration of over 350 mOsm kg⁻¹ by 14 d after the salinity change. Plasma osmolality was unaltered in control fish maintained at 7.5 ppt over the 14-d experiment ($F_{4,35} = 0.890$, $P = 0.480$).

Plasma Cl⁻ concentration also varied over time in patterns dependent on salinity treatment (fig. 1B; $F_{12,55} = 2.885$, $P = 0.069$). These patterns appear to reflect elevated plasma [Cl⁻] in pupfish moved to 35 or 55 ppt and reduced [Cl⁻] in pupfish moved to 0.3 ppt; however, given the limited replicate sizes associated with these [Cl⁻] data ($n = 2–5$ per treatment and time point) resulting from the small plasma volumes obtained from pupfish, no pairwise statistical comparisons were conducted with these data.

Gill NKA Activity and nkaα₁ₐ mRNA Levels

Gill NKA activity was similar among treatments before salinity transfer ($F_{3,28} = 0.419$, $P = 0.741$) but appeared to vary across time in the control (7.5-ppt) treatment ($F_{4,35} = 6.082$, $P = 0.0008$). Post hoc tests revealed that this variation in NKA activity in the control group included a reduction in NKA activity at the 14-d sampling time, compared to the baseline and 8-h sampling times. NKA activity also varied over time in patterns dependent on salinity (treatment × time interaction: $F_{12,140} = 5.661$, $P < 0.0001$; fig. 2A). Gill NKA first showed elevated activity in pupfish transitioned to hyperosmotic environments 4 d after salinity transfer. By 14 d after salinity transfer, however, pupfish in the 35-, 55-, and 0.3-ppt treatments each exhibited elevated NKA activity, compared to 7.5-ppt controls (fig. 2A). Part of this difference may have been due to lower mean NKA activity in controls at 14 d.
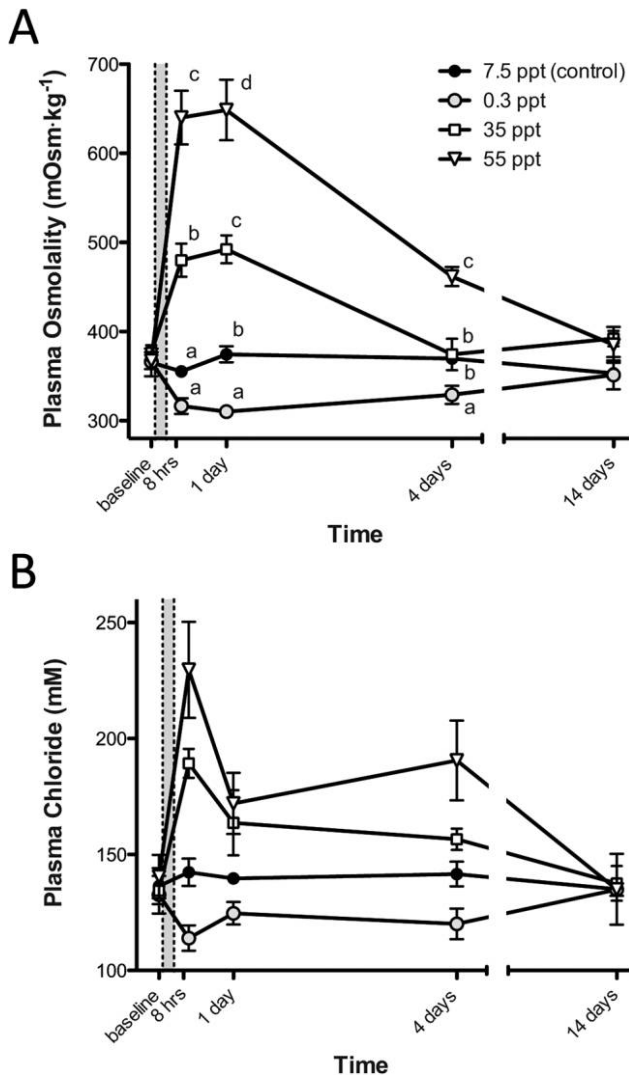
Figure 1. Plasma osmolality (*A*) and chloride ion concentrations ([Cl⁻]; *B*) in pupfish acclimated to 7.5-ppt conditions (baseline) and then either exposed to 0.3 ppt freshwater (gray circles), 35 ppt seawater (squares), or 55 ppt hypersaline water (open triangles) or maintained at 7.5 ppt (control; black circles). The gray area enclosed by dotted lines indicates the period of salinity change (4 h). Data are shown as mean ± SEM. Sample sizes are $n = 7$–8 fish per time point for plasma osmolality and $n = 2$–5 fish per time point for [Cl⁻]. Letters indicate significant pairwise differences between treatments within a given sampling time (Tukey HSD tests). No pairwise statistical tests were run on [Cl⁻] data because of the limited sample sizes of these data.

Gene transcripts encoding $nka\alpha_{1a}$ were similar at the baseline before alteration of environmental salinities ($F_{3,28} = 2.173$, $P = 0.113$) but varied in relative abundance in pupfish exposed to different salinities (fig. 2*B*; $F_{12,140} = 4.143$, $P < 0.0001$). Relative transcript levels of $nka\alpha_{1a}$ in the 7.5-ppt control did not vary across sampling times ($F_{4,35} = 2.025$, $P = 0.112$).

Divergent Responses of Gill NBCe1 Isoform Gene Expression

Transcripts encoding the NBCe1 isoform *nbce1.1* increased in relative expression in the gill of both pupfish exposed to 35-ppt

conditions and those exposed to 55-ppt conditions (fig. 3*A*; treatment × time interaction: $F_{12,140} = 7.5252$, $P < 0.0001$) and remained elevated throughout the 14-d experimental period. However, transcripts encoding NBCe1 isoform *nbce1.2* exhibited a distinctly different pattern and were two- to 2.5-fold higher in fish transferred to 0.3 ppt at 8, 24, and 96 h but then returned to control levels by 14 d (fig. 3*B*; treatment × time interaction: $F_{12,140} = 1.9475$, $P = 0.0336$). Transcripts for *nbce1.2*

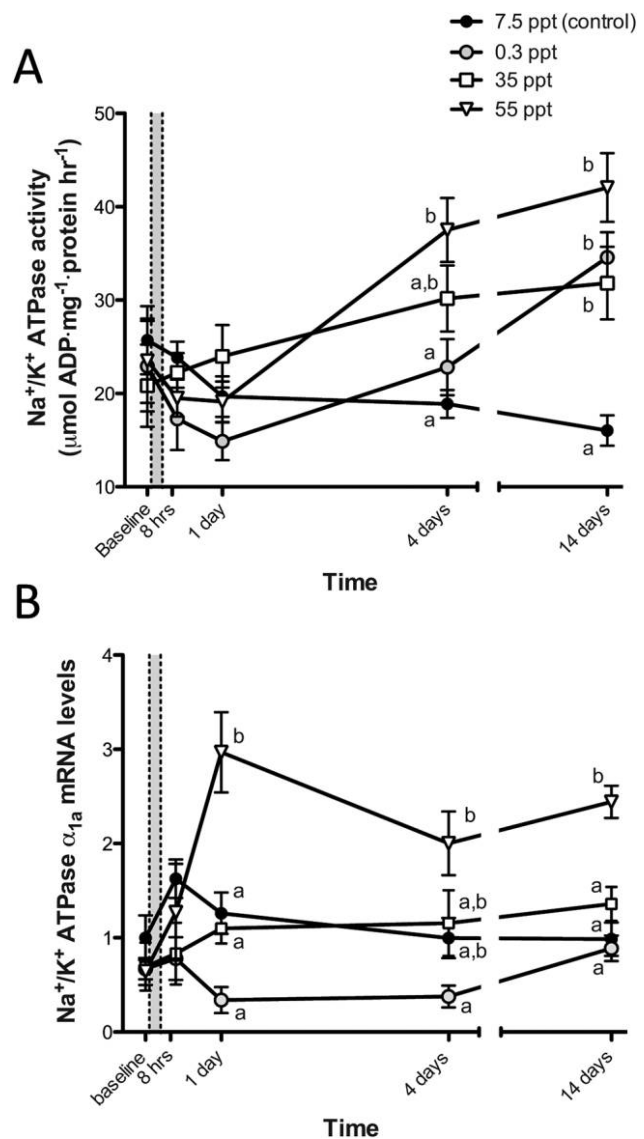Figure 2. Gill Na⁺/K⁺-ATPase activity (*A*) and relative gene transcript abundance for the Na⁺/K⁺-ATPase α_{1a} subunit (*B*) in pupfish acclimated to 7.5-ppt conditions (baseline) and then either transferred to 0.3-ppt freshwater (gray circles), 35-ppt seawater (squares), or 55-ppt hypersaline water (triangles) or maintained at 7.5 ppt (control; black circles). The gray area enclosed by dotted lines indicates the period of salinity change (4 h). Data are shown as mean ± SEM. Sample sizes are $n = 7$–8 fish per sampling time for Na⁺/K⁺-ATPase activity, and $n = 8$ fish for relative messenger RNA (mRNA) levels. Letters indicate significant pairwise differences between treatments within a given sampling time (Tukey HSD tests).
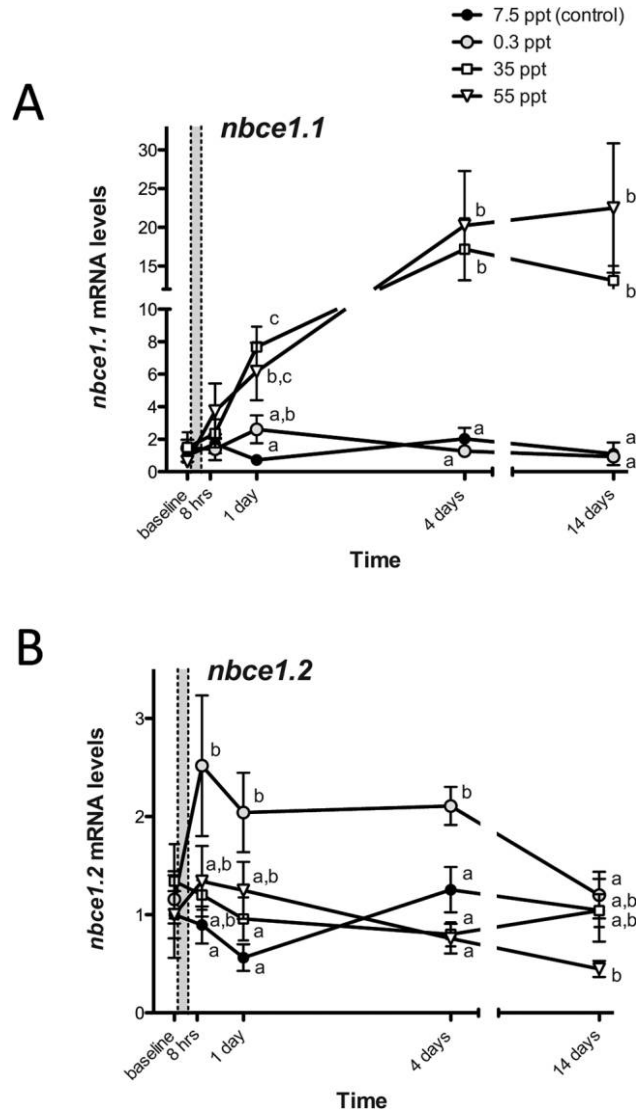
Figure 3. Gill messenger RNA (mRNA) levels of Na^+-HCO_3^- cotransporter-1 isoforms *nbce1.1* (A) and *nbce1.2* (B) of pupfish exposed to salinity change. The gray area enclosed by dotted lines indicates the period of salinity change (4 h). Data are shown as mean ± SEM, with $n = 8$ fish per sampling time. Letters indicate significant pairwise differences between treatments within a given sampling time (Tukey HSD tests).

were also at lower relative levels in the gill of pupfish exposed to 55 ppt for 14 d.

Additional Gill Ion Transporters

There were no differences in relative expression for any of the gill ion transporters among treatment tanks at the baseline sampling time, before commencement of salinity changes (one-factor ANOVA models, range: $P = 0.113–0.885$). Likewise, mRNA levels for all ion transporters were stable in the 7.5-ppt control across all sampling times (one-factor ANOVA models, range: $P = 0.133–0.984$).

Changes in relative mRNA abundance were observed in the gill for some ion transporters after transfer of pupfish from 7.5 ppt to either higher or lower environmental salinities. Gene transcripts encoding *cftr* increased in the gill within 8 h of transfer to both 35- and 55-ppt conditions and remained elevated in these hypersaline treatments throughout the 14-d experiment (fig. 4A; treatment × time interaction: $F_{12,140} = 5.589$, $P < 0.0001$). Transcripts encoding *nkcc1* (gill form; Cutler and Cramb 2002) likewise increased in relative abundance under higher salinity ($F_{12,140} = 5.5977$, $P < 0.0001$; fig. 4B). In contrast, the abundance of transcripts encoding *nkcc2* in the gills was not affected by transfer to either higher- or lower-salinity conditions (fig. 4C).

Transcript abundance for other ion transporters was increased in the gill of pupfish exposed to FW (0.3 ppt; fig. 5). Transcripts for pupfish *ncc2* mRNAs (gill-type slc12a10 paralog; Hsu et al. 2014) were lower in relative expression in fish in the 55-ppt treatment, compared to control (7.5-ppt) fish, by 4 d after salinity transfer and elevated in fish within the 0.3-ppt environment 14 d after transfer (fig. 5A; treatment × time interaction: $F_{12,140} = 4.521$, $P < 0.0001$). Transcripts encoding *v-ATPase* likewise became elevated in the gills of pupfish transferred to 0.3-ppt salinity (fig. 5B). This elevation in relative *v-ATPase* mRNA levels was first apparent 8 h after salinity transfer but gradually became reduced in magnitude until *v-ATPase* transcript abundance was again at control levels by 14 d after transfer.

Gene transcripts encoding two Na^+/H^+ exchangers, *nhe2* and *nhe3*, increased in relative abundance in fish exposed to FW. Gill transcripts for *nhe2* increased rapidly in pupfish transitioned to 0.3 ppt (fig. 5C) but returned to control levels within 4 d in FW (treatment × time interaction: $F_{12,140} = 2.210$, $P = 0.014$). Transcripts encoding *nhe3* also were higher in the gill of pupfish at 0.3 ppt, were observed to be at roughly three- to fourfold higher levels after 24 h in FW (fig. 5D; treatment × time interaction: $F_{12,140} = 5.087$, $P < 0.0001$), and remained elevated over the entire 14-d experiment. Relative carbonic anhydrase (*ca2*) mRNA levels also varied with salinity and were elevated briefly 24 h after the salinity change in 0.3-ppt fish, compared to 35- and 55-ppt fish (fig. 5E). Transcript abundance for *ca2*, however, returned to control levels within 4 d (treatment × time interaction: $F_{12,140} = 2.219$, $P = 0.014$).

Gill ostf1 and Aquaporin mRNA Levels

Gill transcript levels for *ostf1* increased in pupfish transferred to 55 ppt (fig. 6; $F_{12,140} = 4.242$, $P < 0.0001$). This increase was seen only at 8 h, however, as *osft1* transcript abundance quickly returned to control levels 24 h after salinity transfer. No changes in *ostf1* mRNA levels were observed in fish transferred to either 35- or 0.3-ppt conditions.

The abundance of transcripts encoding aquaporin isoform-1 (*aqp1*) in the gill was unaltered by environmental salinity (fig. 7A). Transcripts encoding *aqp3*, however, exhibited significant changes in expression related to salinity (fig. 7B; treatment × time interaction: $F_{12,140} = 13.543$, $P < 0.0001$). Gill mRNA levels for *aqp3* were elevated more than 20-fold in pupfish in the 0.3-ppt
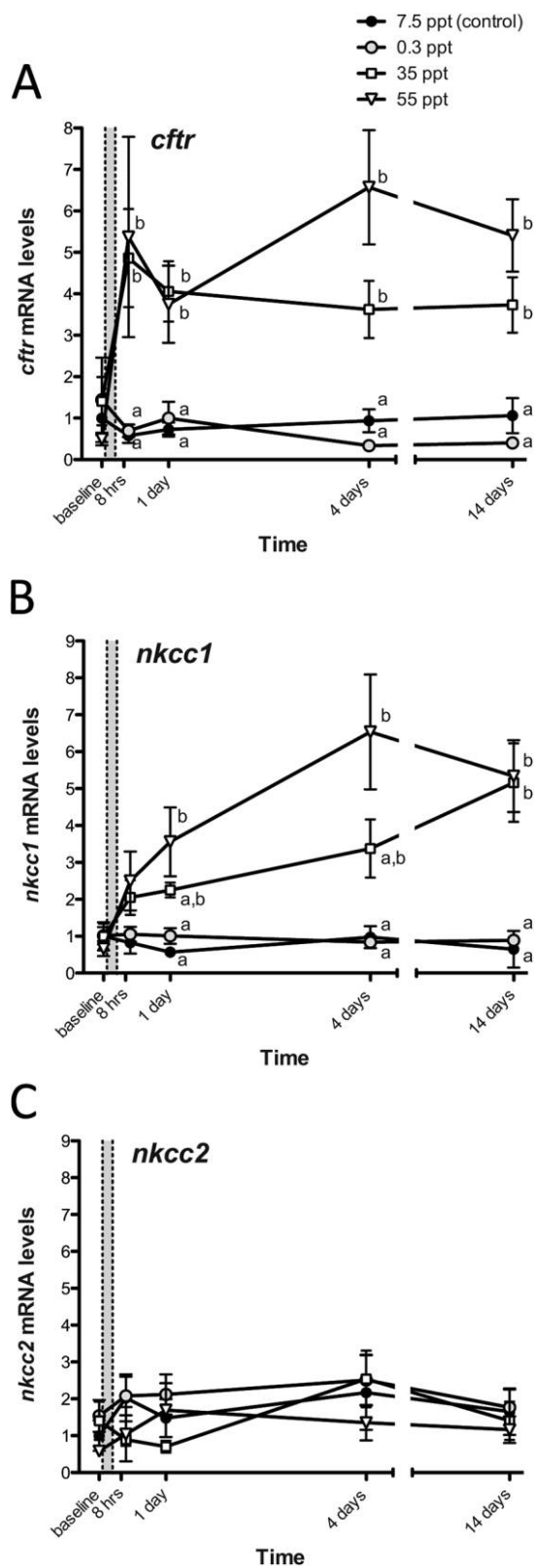
Figure 4. Gill messenger RNA (mRNA) levels for cystic fibrosis transmembrane conductance regulator (*cftr*; *A*), Na$^+$/K$^+$/2Cl$^-$ cotransporter 1 (*nkcc1*; *B*), and Na$^+$/K$^+$/2Cl$^-$ cotransporter 2 (*nkcc2*; *C*) in the gill of pupfish acclimated to 7.5-ppt conditions (baseline) and then transferred to 0.3-ppt freshwater (gray circles), 35-ppt seawater (squares), or 55-ppt hypersaline water (triangles). Control fish were maintained at 7.5 ppt (black circles). The gray area enclosed by dotted lines indicates the period of salinity change (4 h). Data are shown as mean ± SEM, with $n = 8$ fish per sampling time. Letters indicate significant pairwise differences between treatments within a given sampling time (Tukey HSD tests). Transcripts encoding *nkcc2* were unaltered by salinity transfer.

conditions 1 and 4 d after the salinity change and remained roughly fourfold higher than control levels at 14 d. We also observed a transient (at 8 h only) increase of gill *aqp3* mRNAs in pupfish exposed to 55 ppt.

Discussion

Gill NKA Activity and Transcriptional Responses during Acclimation to Hyperosmotic Conditions

The ability of euryhaline fishes to move into higher-salinity environments requires modulation of ion transport across the gills to compensate for the loss of water from tissues and the diffusive gain of ions. In SW-tolerant teleost fishes, changes in NaCl secretion by the gills are mediated by paracellular transport of Na$^+$ and transcellular transport of Cl$^-$, both driven by an active transport NKA in the basolateral membrane of epithelial ionocytes. Changes in ion movement across the gill epithelium therefore involve coordinated shifts in the activity of several transporter proteins as well as regulatory changes in gene expression for these channels and pumps (see fig. 9; e.g., Sardella et al. 2004; Scott et al. 2005; Li et al. 2014).

Within hours of transfer of pupfish from 7.5-ppt conditions to SW (35-ppt) or hypersaline (55-ppt) environments, we observed increases in plasma osmolality and Cl$^-$, indicating that the pupfish were experiencing ion influx and/or water loss. Pupfish transferred from 7.5- to 35- or 55-ppt environments also showed elevated gill NKA activity 4 and 14 d after the salinity change, supporting the idea that regulatory changes in NKA expression in the gill are critical for increasing salt secretion when fish acclimate to hyperosmotic conditions. We also observed an increase in NKA activity at 14 d in pupfish transitioned to FW, suggesting that NKA in the pupfish gill exhibits a U-shaped response pattern with induction at both lower and higher salinities, as has been observed in other fishes (e.g., Jensen et al. 1998; Scott et al. 2004). Transcript abundance for the α$_{1a}$ subunit of NKA (*nkaα$_{1a}$*), however, was elevated only in pupfish transitioned to 55 ppt—and not in those transferred to either 35 or 0.3 ppt. Similar increases in gill *nkaα$_{1a}$* mRNA levels after transfer to higher environmental salinities have been observed in several fish taxa (Richards et al. 2003; Scott et al. 2004; Tipsmark et al. 2011), supporting the role of changes in gill NKA subunit gene expression as one component contributing to increased NKA activity during acclimation to changing salinity. Even so, observed discrepancies in the timing and pattern of NKA activity, compared to *nkaα$_{1a}$* mRNAs, reinforces the importance of considering processes such as posttranscriptional regulation and subunit paralog switching in the modulation of gill NKA activity during salinity acclimation (e.g., McCormick et al. 2009; Tipsmark et al. 2011).
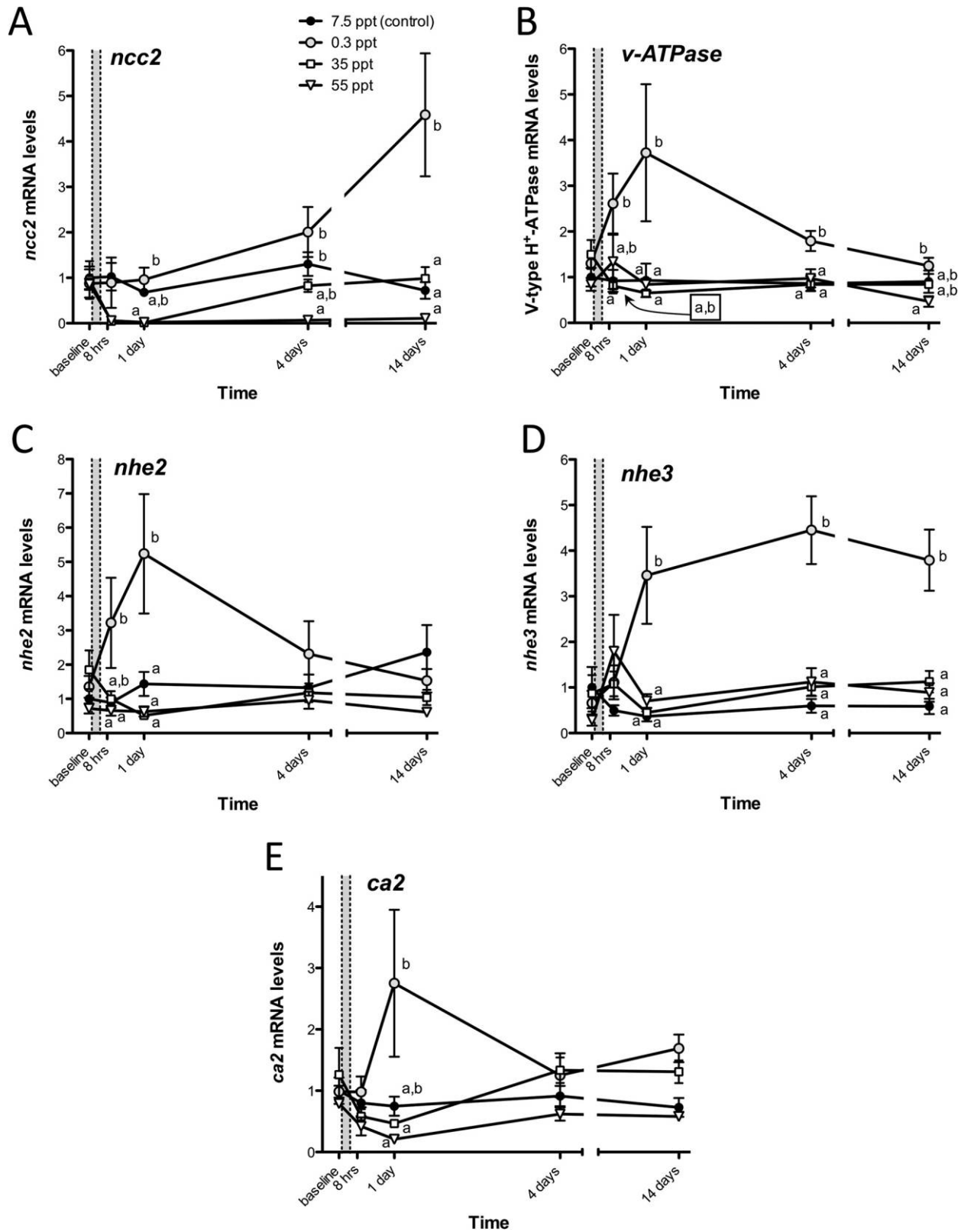
Figure 5. Gill messenger RNA (mRNA) levels for a gill-type (slc12a10) Na^+/Cl^- cotransporter (*ncc2*; *A*), V-type H^+-ATPase β subunit (*v-ATPase*; *B*), Na^+/H^+ exchanger isoform 2a (*nhe2a*; *C*), Na^+/H^+ exchanger isoform 3 (*nhe3*; *D*), and carbonic anhydrase 2-like (*ca2*; *E*) in the gills of pupfish acclimated to 7.5-ppt conditions (baseline) and then transferred to 0.3-ppt freshwater (gray circles), 35-ppt seawater (squares), or 55-ppt hypersaline water (triangles). Control fish were maintained at 7.5 ppt (black circles). The gray area enclosed by dotted lines indicates the period of salinity change (4 h). Data are shown as mean $\pm$ SEM values, with $n = 8$ fish for each treatment and sampling time. Letters indicate significant pairwise differences between treatments within a given sampling time (Tukey HSD tests). Note that the box enclosing letters in *B* indicates the Tukey pairwise comparison designation for the control (black circles) treatment at the 8-h time point.
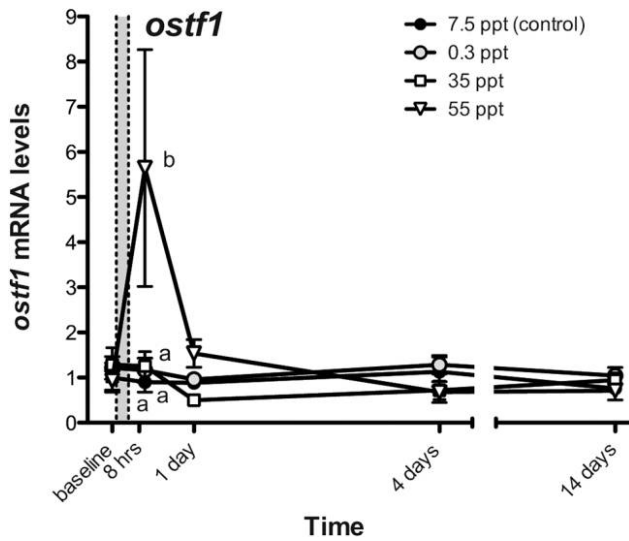
Figure 6. Relative gene transcript abundance of osmotic transcription factor-1 (*ostf1*) in the gill epithelium of pupfish acclimated to 7.5-ppt conditions (baseline) and then exposed to 0.3-ppt freshwater (gray circles), 35-ppt seawater (squares), or 55-ppt hypersaline water (triangles). Control fish were maintained at 7.5 ppt (black circles). The gray area enclosed by dotted lines indicates the period of salinity change (4 h). Data are shown as mean $\pm$ SEM, with $n = 8$ fish for each treatment and sampling time. Letters indicate significant pairwise differences between treatments within a given sampling time (Tukey HSD tests). mRNA = messenger RNA.

Gill NKA activity has similarly been shown to increase after transfer of the Salt Creek pupfish (*Cyprinodon salinus*) from 12-ppt to FW, SW (35-ppt), or hypersaline (112-ppt) conditions (Stuenkel and Hillyard 1980). Euryhaline mummichog acclimated to higher environmental salinities likewise exhibit elevated epithelial NKA activity (Epstein et al. 1967; Towle et al. 1977), which maintains a low Na$^+$ concentration in the ionocyte. Accordingly, fish transferred from FW to SW similarly show increased NKA activity within minutes (Mancera and McCormick 2000), likely as a result of activation of protein already in the membrane, which is followed by a delayed increase in NKA subunit mRNA levels 2–3 d after SW transfer (Scott and Schulte 2005). The NKA protein is positioned basolaterally in ionocytes in the mummichog gill epithelium (Karnaky et al. 1976), so that Cl$^-$ secretion by ionocytes requires the action of other transporter proteins positioned apically, such as Cftr (fig. 9; e.g., Edwards and Marshall 2013).

More recently, several studies provide evidence for NKAα1-subunit switching in the gill during salinity acclimation. NKA is composed of α and β subunits (and in some cases a λ subunit; Garty and Karlish 2006), with the α subunit mediating the catalytic activity via binding sites for Na$^+$, K$^+$, and ATP (Jorgensen et al. 2003). Recent studies in rainbow trout, Atlantic salmon (*Salmo salar*), Mozambique tilapia (*Oreochromis mossambicus*), and alewife (*Alosa pseudoharengus*) identified distinct, salinity-specific α1-subunit isoforms, which originate from apparently independent evolutionary events (Richards et al. 2003; Nilsen et al. 2007; Tipsmark et al. 2011; Velotta et al.

2017; see also Blondeau-Bidet et al. 2016). Richards and colleagues (2003) observed increased gill $nka\alpha_{1a}$ isoform mRNA levels after transfer of rainbow trout from SW to FW but increases in the $nka\alpha_{1b}$ isoform after transfer from FW to SW. Tipsmark et al. (2011) likewise found evidence for isoform switching in the tilapia gill, with SW-acclimated fish exhibiting increased $nka\alpha_{1a}$ mRNA levels and decreased $nka\alpha_{1b}$ mRNA levels after transfer to FW. Using isoform-specific antibodies for immunohistochemistry, McCormick and coworkers (2009) detected differences in α1-subunit protein expression and distribution in the gill epithelium of Atlantic salmon parr, with NKAα_{1a} levels prevalent in filamental and lamellar ionocytes of
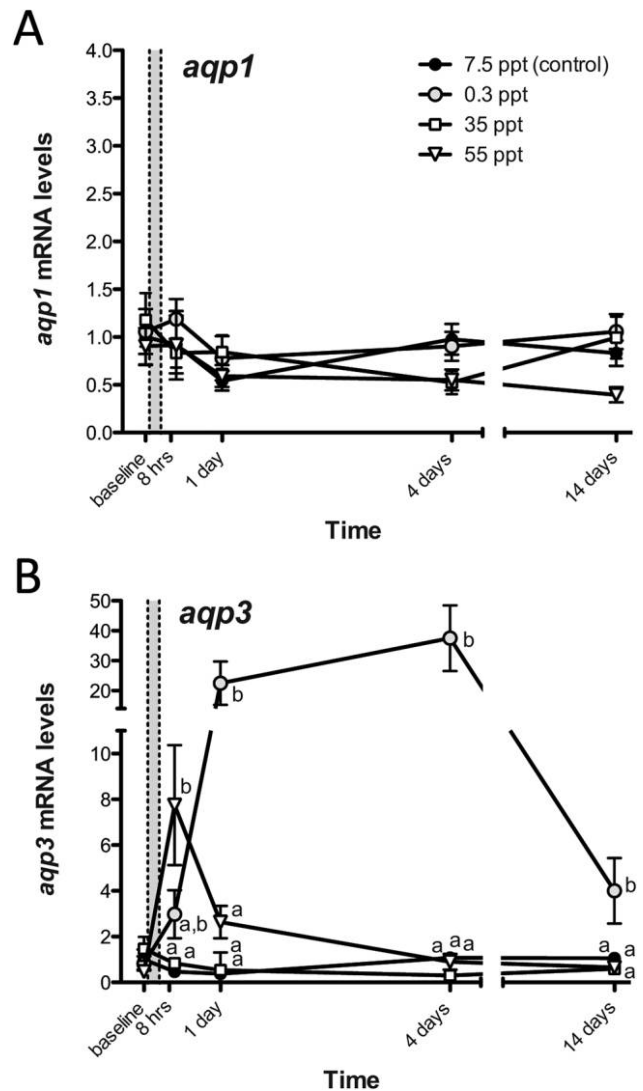
Figure 7. Gill messenger RNA (mRNA) levels for aquaporin-1 (*aqp1*; *A*) and aquaporin-3 (*aqp3*; *B*) in pupfish acclimated to 7.5-ppt conditions (baseline) and then transferred to 0.3-ppt freshwater (gray circles), 35-ppt seawater (squares), or 55-ppt hypersaline water (triangles). Control fish were maintained at 7.5 ppt (black circles). The gray area enclosed by dotted lines indicates the period of salinity change (4 h). Data are shown as mean $\pm$ SEM, with $n = 8$ fish for each treatment and sampling time. Letters indicate significant pairwise differences between treatments within a given sampling time (Tukey HSD tests).

parr in FW, but NKAα_{1b} protein predominating in SW. To date, we have been unable to identify multiple isoforms of $nka\alpha_1$ subunit in Amargosa pupfish, but the question of whether multiple $nka\alpha_1$ isoforms also evolved in this taxon—and whether any such isoforms vary in expression patterns during salinity changes—should be explored in future studies.

Our finding that mRNAs encoding $cftr$ and the gill paralog of $nkcc1$, but not $nkcc2$, increased two- to sixfold in the gill 8–24 h after transfer of pupfish to higher salinities supports the involvement of the Cftr channel and the Nkcc1 transporter in NaCl secretion. Basolaterally located Nkcc1 moves Cl^- into the ionocyte from the blood to maintain ionocyte Cl^- concentrations above electrochemical equilibrium, while the Cftr channel—which is positioned apically in mummichog (Marshall et al. 2002; Katoh and Kaneko 2003)—facilitates Cl^- movement to the external environment. Nkcc1 activity increases via protein phosphorylation after transfer of *Fundulus heteroclitus* to higher salinities (Flemmer et al. 2010), and the abundance of transcripts encoding $nkcc1$ and $cftr$—but not $nkcc2$, which functions largely in ion transport in intestinal and renal tissues—increases in the gill of mummichog and other euryhaline or brackish-tolerant fishes (e.g., *Oreochromis* sp., *Oryzias* sp., *Dicentrarchus labrax*) transferred to hyperosmotic conditions (Singer et al. 1998; Scott et al. 2004, 2008; Tse et al. 2006; Hiroi et al. 2008; Shaw et al. 2008; Bodinier et al. 2009; Kang et al. 2010; Berdan and Fuller 2012; Li et al. 2014), which is consistent with the results of our study.

Distinct mRNA Responses of Teleost NBCe1 Isoforms

In mammals, the Na^+-HCO_3^- cotransporter is encoded by a single gene, $slc4a4$ (Romero et al. 2013). In teleost fishes, however, the $slc4a4$ gene underwent a duplication event, so that at least some teleost fishes appear to possess two distinct genes encoding the putative Na^+-HCO_3^- cotransporters referred to as NBCe1.1 and NBCe1.2 (fig. 8). That duplication was first identified by Lee and coworkers (2011), who isolated two distinct $slc4a4$ genes ($zslc4a4.1$ and $zslc4a4.2$) in zebrafish. Subsequent work by Chang et al. (2012) revealed that duplicated $slc4a4$ genes are prevalent across a wide variety of Actinopterygii fishes, with several species expressing mRNA splice variants of one or both genes. Our own phylogenetic analysis confirmed the broad taxonomic distribution of two NBCe1 forms across teleosts. Interestingly, our phylogenetic analyses confirm the identity of two $slc4a4$ isoforms in pupfish and also indicate that there are more than two NBCe1.2 isoforms in salmoniform fishes (fig. 8), implying a second duplication of the $slc4a4.2$ gene in that lineage.

Our data provide evidence for distinct patterns of gene expression responses for these two NBCe1 isoforms in the gill during salinity challenge. Transcripts encoding the $nbce1.1$ form showed elevated gill expression in pupfish transferred to hypersaline environments (35 or 55 ppt), with mRNA levels increasing six- to eightfold within 24 h of transfer and remaining elevated as much as 22-fold even after 14 d in the higher-salinity environments. In contrast, the abundance of gene transcripts encoding the NBCe1.2 isoform increased in

the gill of pupfish transferred from 7.5- to 0.3-ppt conditions; $nbce1.2$ mRNA levels in those fish increased after 8 h of salinity transfer and remained elevated at least 4 d after the salinity change.

In 5-dpf (days postfertilization) embryos of the stenohaline zebrafish (*Danio rerio*), mRNAs for NBCe1.2 (termed zNBCe1b by the authors) colocalized with transcripts encoding Ncc in the yolk sac, suggesting that NBCe1.2 is expressed in Ncc-type ionocytes, at least in that tissue and developmental stage (Lee et al. 2011). In adult zebrafish, transcript abundance for NBCe1.2 was elevated in the gills of fish exposed to a higher-$[Na^+]$ (10-mM) environment, compared to those of fish exposed to a low-$[Na^+]$ (0.04-mM) environment (Lee et al. 2011). In the same study, gill mRNA levels for NBCe1.2 were also found to be lower in fish exposed to acidic (pH 4.00–4.05) conditions than in fish in a near-neutral pH environment (pH 6.7–6.9; Lee et al. 2011). That study, however, did not examine the expressional regulation of the other isoform, NBCe1.1. Given that the 7.5-ppt (control, pH 7.68) and 0.3-ppt (pH 7.66) treatments used in our study with pupfish varied only slightly in pH conditions, we interpret the elevated gill $nbce1.2$ mRNA abundance in the 0.3-ppt fish as being related to the osmotic conditions and not a change in environmental pH.

In mummichog, however, mRNA levels for $nbce1$ in the gill were unaffected by transfer of fish to lower salinity (Scott et al. 2005). For this work, Scott and colleagues (2005) cloned and sequenced a 94-bp nucleotide partial cDNA of Nbc1 (AY796058), which our BLAST analyses indicate was encoding the NBCe1.2 isoform (XM_012853007). Kurita et al. (2008) held mefugu (*Takifugu obscurus*) maintained under FW or SW conditions for 8 d and observed no differences in gill NBCe1 mRNA levels, although it is unclear which NBCe1 isoform was examined.

Our results provide the first evidence demonstrating isoform-specific patterns of transcriptional regulation of the Na^+-HCO_3^- cotransporter (NBCe1) in the teleost gill. While the patterns of hypoosmotic induction of NBCe1.2 that we observed generally agree with the previously proposed role of a basolateral NBCe1 protein functioning in acid-base regulation—and possibly basolateral Na^+ movement from the cytoplasm to the serosal side of ionocytes (e.g., Parks et al. 2007)—in teleosts in FW environments, our observation of approximately 20-fold increases in mRNA levels encoding $nbce1.1$ in pupfish under hyperosmotic conditions suggests a distinct role for NBCe1.1 in regulating ionic or acidic balance in high-salinity environments. Such distinct patterns of NBCe1 isoform regulation in hypo- and hyperosmotic environments provide evidence for salinity-dependent "isoform switching," which has previously been shown only for the NKA α subunit. Future studies should develop immunohistological assays that can distinguish these two NBCe1 isoforms to confirm the localization of these proteins in ionocytes and confirm that changes in mRNA levels indeed translate into changes in NBCe1 isoform protein expression. Given the dissimilar salinity-dependent mRNA responses observed here, it appears that NBCe1 shows isoform switching in the gill in response to hypo- or hyperosmotic conditions. An important area of future research will be to examine
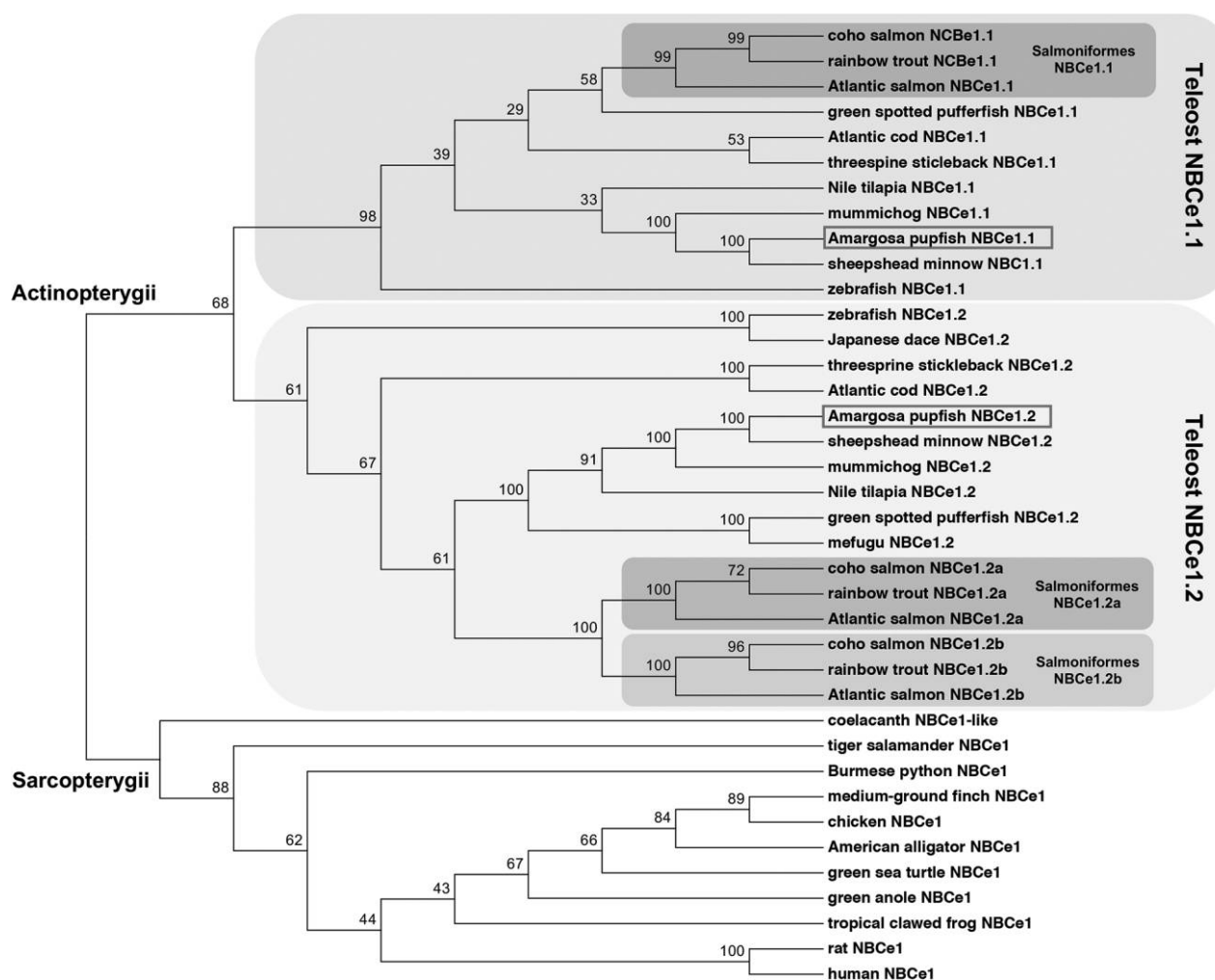
Figure 8. Phylogenetic analysis of electrogenic Na^+-HCO_3^- cotransformer-1 (NBCe1) proteins in teleost fishes. Amino acid sequences were aligned in Clustal X software (Larkin et al. 2007), and a consensus phylogenic tree was constructed with a neighbor-joining Tamura-Nei model with all sites (MEGA v7 software; Kumar et al. 2016). Bootstrap values represent 1,000 replicates. Two NBCe1 genes have evolved in teleost fishes, NBCe1.1 and NBCe1.2. Boxes denote the NBCe1.1 and NBCe1.2 paralogs of Amargosa pupfish (*Cyprinodon nevadensis*) examined in this study. Note also the presence of an additional duplication of the NBCe1.2 isoform in salmonid fishes (order Salmoniformes). GenBank or Ensembl accession numbers for Amargosa pupfish sequences are as follows: NBCe1.1 (*C. n. amargosae* spp.: KT162090; *C. n. pectoralis* spp.: JSUU01027575, JSUU01007559, JSUU01000712, JSUU01014542, and JSUU01030693); NBCe1.2 (*C. n. pectoralis*: JSUU01000712 and JSUU01094524). GenBank or Ensembl accession numbers for amino acid sequences of putative NBCe1 proteins from other taxa are provided in table A3. A color version of this figure is available online.

whether the two NBCe1 protein isoforms localize to different cell types or membrane regions, as well as whether these isoforms show differences in ion kinetics or endocrine regulation. That additional information should provide a clearer picture of how these the two teleost NBCe1 transporters may be differentially mediating osmo- and ionoregulatory responses of the gill to salinity change.

Induction of ostf1 Gene Expression in Hyperosmotic Environments

For pupfish transferred to 55 ppt, the increase in plasma osmolality was paralleled by a transient, nearly sixfold increase in gill *ostf1* mRNA levels. Ostf1, also termed TSC22 domain family protein 3, was initially identified as a rapidly upregulated transcript by use of suppressive subtractive hybridization comparisons of gill mRNA expression in FW- and SW-acclimated Mozambique tilapia (Fiol and Kültz 2005) and has since been classified as an osmosensing molecule in teleost fishes (Kültz 2005, 2013; Tse 2014). Ostf1 is thought to be a transcription factor on the basis of its leucine zipper DNA domain, but the precise gene targets of Ostf1 in teleosts remain unknown. In euryhaline fishes, both mRNA and protein levels of Ostf1 in the gill epithelium are induced by hyperosmotic salinity (e.g., Fiol et al. 2006; Fiol and Kültz 2007; Choi and An 2008; Breves et al. 2010; Chow and Wong 2011; Tse et al. 2011), with Ostf1 protein

expressed highly in ionocytes (Tse et al. 2012). In the Mozambique tilapia, transfer of fish from FW to SW (1,000 mOsm kg^{-1}) resulted in a nearly sixfold induction of *ostf1* mRNA levels 1–4 h after salinity transfer, followed by increased Ostf1 protein at 4–6 h after transfer (Fiol and Kültz 2005).

Our results here indicate that pupfish experienced a rapid (8-h) increase in relative *ostf1* mRNA levels in the gill epithelium after transition from 7.5 to 55 ppt, which supports the proposed role of Ostf1 as an osmosensor molecule to hyperosmotic stress (Kültz 2013). As expected, we did not observe any change in gill *ostf1* mRNA levels when pupfish were transferred from 7.5 to 0.3 ppt. Why we did not observe an increase in *ostf1* mRNAs in pupfish exposed to 35 ppt, however, is not clear. Salinity-induced increases in gill *osft1* transcript abundance are transitory; in tilapia, for example, a roughly sixfold increase in gill *ostf1* was observed 1 h after transfer from FW to SW, but *ostf1* had returned to baseline, pretransfer levels within 8 h after transfer. It is therefore possible that the first posttransfer sampling time of 8 h used in our current study was too late to detect a transitory increase in *ostf1* mRNAs in the 35-ppt treatment group but that the *ostf1* mRNA increase in the 55-ppt group was either greater in magnitude or longer in duration.

While it is not entirely known which genes are regulated by Ostf1 in the fish gill, ectopic expression of Ostf1 induced gene transcription for *cftr*, *nhe3*, and *aqp1* in human kidney HEK293 cells (Tse et al. 2011). Similarly, morpholino knockdown of *ostf1* (b isoform) decreased both *cftr* and *aqp1* mRNA abundance in the gill of the medaka (*Oryzias latipes*; Tse et al. 2011), suggesting that Ostf1 functions in osmosensory signal transduction via transcriptional regulation of select ion transporters and aquaporins. While we did not test for any direct effects of Ostf1 on ion transporter or aquaporin regulation in pupfish, we did observe increases in the abundance of mRNAs encoding *cftr* in the gills within 8 h of transfer of pupfish to 35- or 55-ppt conditions, followed by increases in gill *nkcc1*, *nbce1.1*, and *nkaα$_{1a}$* transcript abundance by 24 h. Ion secretion from the gill of the related cyprinodontoid fish mummichog increases within a few hours after transfer of fish from fresh or brackish conditions to SW (Wood and Laurent 2003; Prodocimo et al. 2007; Wood and Grosell 2008), and patterns of mRNA abundance changes observed here in pupfish are consistent with the hypothesis that transcriptional upregulation of *cftr*, *nkcc1*, *nbce1.1*, and *nkaα$_{1a}$* contributes to the excretion of excess ions and return of plasma osmolytes to homeostatic concentrations.

Gill Transcription Responses to a Hypoosmotic Environment

Acclimation of teleosts to FW requires coordinated changes in membrane transporters for ion uptake and acid-base regulation (Evans et al. 2005). As mentioned above, we observed elevated NKA activity in the gill 14 d after pupfish were transitioned to FW. Similar increases in gill NKA activity have been observed in other fishes during acclimation to low-salinity conditions (e.g., Jensen et al. 1998; Scott et al. 2004). In other fishes, those FW-induced increases in gill NKA activity have been linked to increases in NKA protein expression and NKA α$_1$-subunit

switching (Richards et al. 2003; McCormick et al. 2009; Tipsmark et al. 2011). We were unable to identify two NKA α$_1$ subunits in pupfish in our study; however, the possibility that pupfish have also evolved multiple α$_1$ subunits might help explain why we did not observe any changes in gill *nkaα$_{1a}$* mRNA levels in pupfish transitioned to FW.

While several models have been proposed for gill ion regulation in FW (e.g., Edwards and Marshall 2013), it is thought that a V-type H$^+$-ATPase enzyme coupled electrogenically to a Na$^+$ channel contributes to Na$^+$ uptake and acid secretion by the gills of many teleosts (see fig. 9). While expressed in a variety of gill ionocytes and respiratory pavement cells (e.g., Lin et al. 1994; Sullivan et al. 1995, 1996), the location of this V-type H$^+$-ATPase, however, appears to vary across taxa. In trout, V-type H$^+$-ATPase is present in the apical membrane (Lin et al. 1994), while in mummichog, the V-type H$^+$-ATPase enzyme is expressed in the basolateral membrane (Katoh et al. 2003). Even so, H$^+$-ATPase likely functions in combination with shifts in the expression or activity of NKA, carbonic anhydrase, and Na$^+$/H$^+$ exchangers Nhe2 and Nhe3 (e.g., Lin et al. 2008). Relatively few studies have been conducted to date in pupfishes, but recent data from Brix and Grosell (2013) pointed toward a low-affinity Nhe cotransporter coupled to H$^+$ production by carbonic anhydrase involved in Na$^+$ uptake in low-Na$^+$ environments in the desert pupfish *Cyprinodon macularius*.

We observed that pupfish transferred from 7.5- to 0.3-ppt conditions had elevated gill mRNAs encoding *v-ATPase*, *ca2*, *nhe2*, and *nhe3*. Pupfish transferred to 0.3 ppt expressed elevated mRNA levels for *v-ATPase* and *nhe2* within 8 h of salinity change, and levels of both these transcripts peaked as roughly four- to sixfold increases at the 1-d sampling time before declining toward control levels by 4 d (*nhe2*) or 14 d (*v-ATPase*). Gene transcripts encoding *ca2* and *nhe3* were also elevated by 1 d after transfer to lower salinity; *ca2* mRNAs returned to control levels by 4 d, while *nhe3* transcripts remained elevated roughly three- to fourfold through the duration of the 14-d period after salinity transfer.

Transcriptional changes in each of these genes have been documented previously in the gills of teleosts transferred to lower-salinity environments. Scott and coworkers (2005) observed a transient elevation in gill *nhe2* mRNAs 12 h after transfer of mummichog from 10% SW to FW; *nhe2* mRNA levels, however, were similar to those of 10%-SW fish at sampling times 3 or 7 d after FW transfer, indicating that the increase in gill *nhe2* mRNAs under hypoosmotic conditions is temporary, as we also observed here in pupfish. Unlike our findings here, however, Scott et al. (2005) observed a decrease in gill *nhe3* mRNAs in mummichog transferred to FW. Why that pattern differed from the one observed for *nhe3* here is not clear. Inokuchi and coworkers (2008) observed elevated gill *nhe3* mRNAs in Mozambique tilapia transferred to an FW environment for 7 d, and Moorman et al. (2014, 2015) likewise observed elevated gill *nhe3* mRNAs in this same species in FW, similar to our findings with pupfish. Seo and coworkers (2013) also observed elevated Nhe3 protein and mRNA expression in the ionocytes of Japanese eel (*Anguilla japonica*) in FW. Even so, some species of
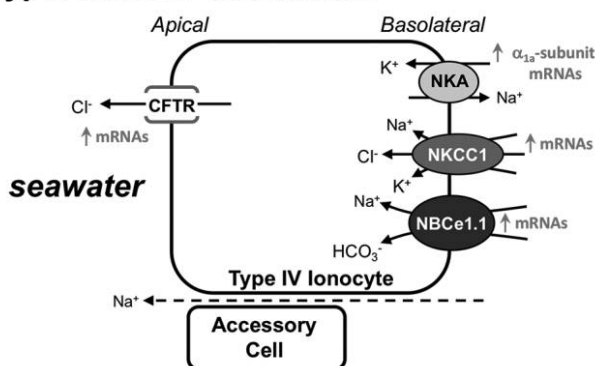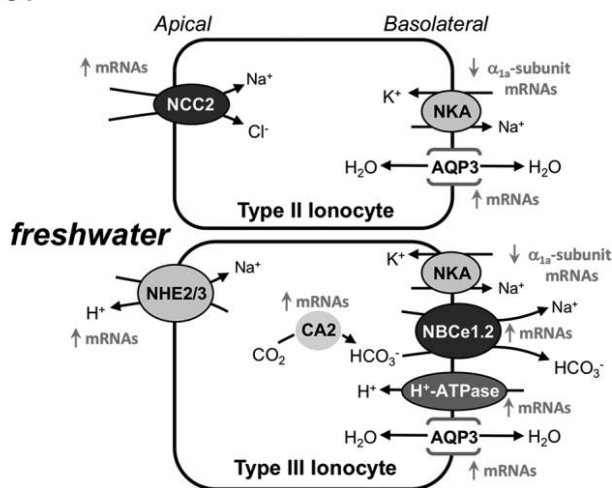
Hyperosmotic Conditions:

Hypoosmotic Conditions:

Figure 9. Illustration of proposed membrane positions and functional roles of proteins observed to change in gene transcript abundance in the pupfish gill after transition to either hyperosmotic (i.e., 35- or 55-ppt) or hypoosmotic (0.3-ppt [freshwater]) conditions. The proposed distribution of transporter and channel proteins on different types of gill ionocytes is shown. Gray text indicates the direction of changes observed in relative messenger RNA (mRNA) levels for each protein in the pupfish gill during acclimation to hyper- or hypoosmotic conditions. Note that the localization of NBCe1.1 in the basolateral membrane of type IV ionocytes is hypothesized and that while the Aqp3 proteins have been localized to the basolateral ionocyte membrane in fishes (e.g., Lignot et al. 2002; Brunelli et al. 2010; Madsen et al. 2015), it remains unknown which type(s) of ionocytes express Aqp3. This illustration is based on models for gill ionocyte function proposed by Yan et al. (2007), Hwang et al. (2011), and Hiroi and McCormick (2012). A color version of this figure is available online.

teleosts have evolved multiple forms of Nhe3 (e.g., Yan et al. 2007; Ivanis et al. 2008), and it possible that different *nhe3* forms exhibit different regulatory patterns. Alternatively, Edwards and colleagues (2005) observed increased gill Nhe3 protein levels in SW-adapted mummichog exposed to hypercapnic conditions, and variation among experimental designs in other environmental variables might contribute to different *nhe3* mRNA response profiles.

Elevated *ncc* mRNA levels have likewise been observed previously in the gill of tilapia acclimated to FW, compared to those in SW or hypersaline conditions (Inokuchi et al. 2008; Li et al. 2014; Moorman et al. 2014, 2015). Such increased *ncc* mRNA levels likely indicate an increase in Ncc expression in select types of ionocytes in hypoosmotic environments. Hiroi and coworkers (2008) proposed that one type of ionocyte expresses Ncc apically as part of a Na^+ and Cl^- uptake mechanism in FW. Whether the upregulation of *ncc* observed here with pupfish represents an upregulation of this gene to support a large apical surface area for Na^+ and Cl^- uptake in FW or an increase in Ncc-expressing ionocyte number in the epithelium is not clear. In either case, the increased *ncc2* mRNA levels observed in the gill of pupfish in the 0.3-ppt treatment suggests that changes in ionocyte Na^+ and Cl^- transport likely play an important role in the acclimation of pupfish to FW (but see Brix and Grosell 2012).

Beyond changes in ion channel expression, we also observed increased gill *aqp3*—but not *aqp1*—mRNA abundance in pupfish transferred to 0.3 ppt. Levels of *aqp3* mRNA were elevated as much as 30-fold in the gill epithelium in pupfish 1 and 4 d after transfer to lower salinity. Recent studies provide evidence that changes in aquaporin expression in ionocytes may also be important during acclimation to some salinity changes (e.g., Cutler et al. 2007; Giffard-Mena at al. 2007). Branchial *aqp3* gene expression has been shown to be elevated in fish in FW compared to those in SW (Watanabe et al. 2005; Tipsmark et al. 2010; Whitehead et al. 2010; Jung et al. 2012; Moorman et al. 2014, 2015; Breves et al. 2016), and recent studies in tilapia have revealed that gill *aqp3* expression is upregulated by prolactin but that those effects of prolactin can be blocked by cortisol (Breves et al. 2016).

In several fishes, Aqp3 colocalizes with NKA to the basolateral membrane of ionocytes (Lignot et al. 2002; Brunelli et al. 2010; Madsen et al. 2015). Although the functional role of Aqp3 in these cells is not clear, it has been hypothesized that gill Aqp3 expression may function in cell volume regulation or nitrogen metabolism (Kolarevic et al. 2012; Madsen et al. 2015). Aqp3 from zebrafish and European eel is permeable to urea (MacIver et al. 2009; Tingaud-Sequeira et al. 2010), and Aqp3 may function to transport urea in FW, even if another urea-specific transporter functions in this role in SW (e.g., Mistry et al. 2001). What is clear is that future studies are needed to determine the functions for Aqp3 in the teleost gill.

Conclusion

Taken as a whole, our findings here provide a detailed profile of the changes in ion-transporter and aquaporin gene expression that occur in the gill epithelium of a desert pupfish acclimating to changing salinities. Some of these pupfishes' desert habitats experience rapidly shifting salinities during flood events, and the taxa that occupy those habitats need to maintain osmotic and ionic balance under those changing conditions. Maintenance of body-fluid osmolality under those conditions is likely to involve coordinated changes in ion and water movement across the gills, which may be triggered by osmosensing mech-

anisms such as *ostf1*. The results of our study document the time course for transcriptional upregulation of gill ion transporters *nkcc1*, *cftr*, and *nbce1.1* during transitions of pupfish to hyperosmotic conditions, and of *nbce1.2*, *v-ATPase*, *ca2*, *nhe2*, *nhe3*, *ncc2a*, and *aqp3* when pupfish experience hypoosmotic conditions (fig. 9). That observation of distinct patterns of transcriptional regulation for *nbce1.1* and *nbce1.2* points to a possible functional divergence for these two NBCe1 isoforms in acclimation to higher- or lower-environmental-salinity conditions. Given that the evolutionary duplication of NBCe1 into these two isoforms is present across a wide taxonomic variety of teleosts, future work in other euryhaline fishes should explore these two NBCe1 isoforms further for their functional roles in osmo- and ion regulation by the teleost gill.

Acknowledgements

APPENDIX

Material and Methods

Degenerate Primer Design for Amplification and Sequencing of Partial cDNAs

Degenerate primers for *nkaα₁ₐ* were designed to consensus nucleotide regions of *nkaα₁ₐ* cDNAs from the mummichog *Fundulus heteroclitus* (GenBank accession no. AY057072) and blackchin tilapia *Sarotherodon melanotheron* (GU252208), as well as several unannotated expressed sequence tags (ESTs) identified from the guppy *Poecilia reticulata* (ES375881, ES380431, and ES378665). The coding regions of sequences were aligned with Sequencher v5.1 software. Degenerate primers for *nkcc1* were designed to consensus regions for this gene from *F. heteroclitus* (AY533706, DR442079, and GT098098), *Oryzias dancena* (GQ862972), and European seabass *Dicentrarchus labrax* (AY954108), and primers for *nkcc2* were designed to consensus sequence regions of cDNAs from *F. heteroclitus* (AY533707), *P. reticulata* (ES378149), and Mozambique tilapia *Oreochromis mossambicus* (AY513739).

Degenerate primers for *nbce1* were designed to aligned cDNA sequences from *F. heteroclitus* (GQ376030), Nile tilapia (*Oreochromis niloticus*; XM_003444476), and Gulf toadfish (*Opsanus beta*; FJ463158) and those for *cftr* to cDNAs from

F. heteroclitus (AF000271), *D. labrax* (DQ501276), and climbing perch (*Anabas testudineus*; JN180943). Degenerate primers for *nhe2* were designed to consensus regions of previously published cDNA sequences from mummichog (AY818824), Japanese medaka (*Oryzias latipes*; XM_004073656), and *O. niloticus* (XM_003455783), and those for *nhe3* on the basis of cDNA sequences obtained from *Cyprinodon variegatus* (HM142345), *F. heteroclitus* (AY818825 and DR046872), *O. mossambicus* (AB326212), and longhorn sculpin *Myoxocephalus octodecemspinosus* (EU909191). Degenerate primers for *ca2* were designed to *F. heteroclitus* (AY796057; EST sequence GT097731), *O. niloticus* (XM_003439275), and emerald rockfish *Trematomus bernacchii* (GQ443602).

Degenerate primers for *ostf1* were designed to consensus regions of an annotated cDNA from *Tetraodon nigroviridis* (CR690809) and unannotated EST sequences identified from *F. heteroclitus* (CN983552 and DR397775), *P. reticulata* (ES376413), and *Poeciliopsis turneri* (HO911905). Finally, degenerate primers for *aqp1* were designed to sequences from *F. heteroclitus* (EU780153), seabream (*Sparus aurata*; AY626939), and stinging catfish (*Heteropneustes fossilis*; HM051492) and those for *aqp3* to *F. heteroclitus* (EU780154), *D. labrax* (DQ647191), and *O. mossambicus* (AB126941). A set of gene-specific primers was also designed for *v-ATPaseβ* from the pupfish *C. variegatus* (HM142343); these primers were forward 5′-TTCCTCAACCTCGCCAATG-3′ and reverse 5′-TCATTCGGCATCGTCAGAATAG-3′.

Degenerate primers were also designed to amplify a partial cDNA sequence of a thiazide-sensitive Na⁺/Cl⁻ cotransporter (*ncc*; solute carrier family 12 member 3, *slc12a3*) from the pupfish gill. First, a nested set of degenerate primers (listed as "[*ncc*]-like" primers in table A1) was designed to consensus regions of an unannotated EST from turquoise killifish *Nothobranchius furzeri* (JZ229878), a predicted *slc12a3*-like transcript sequenced from zebra mbuna *Maylandia zebra* (XM_004575787), and a predicted *slc12a3*-like transcript from sequenced genome scaffold JH556669 of southern platyfish *Xiphophorus maculatus* (XM_005796245). Gel electrophoresis revealed that these primers amplified a single, faint PCR product from the gill of *Cyprinodon nevadensis amargosae* pupfish, which produced a 344-bp nucleotide sequence (KT162100) that has high deduced amino acid sequence identity to predicted *slc12a3*-like sequences from the other cyprinodontid fishes *X. maculatus* (XM_005796245) and Amazon molly *Poecilia formosa* (XM_007558544). Three different qPCR assays designed to this pupfish cDNA sequence failed to amplify any cDNA products in the pupfish gill with QRT-PCR. Given those initial data, we hypothesized that this pupfish *slc12a3*-like cDNA encodes a *slc12a3*-like paralog expressed in tissues other than the gill and may have been amplified from the pupfish gill only as a result of residual DNA remaining even after DNase I treatment of extracted RNA.

We therefore used the open reading frame of the *scl12a10.2* mRNA of *Danio rerio* (EF591989), which has been shown to encode a gill Na⁺/Cl⁻ cotransporter with osmoregulatory functions in this species (Wang et al. 2009), to BLAST search (http://blast.ncbi.nlm.nih.gov/) and identify additional predicted transcript sequences from *X. maculatus* (XM_005809180) and *M. ze-*

bra (XM_004563490), which were then used to design a second set of nest degenerate primers. These degenerate primers are listed as the *ncc* primers in table A1. This second set of degenerate primers amplified a 1,048-bp nucleotide cDNA sequence from the gill of *C. n. amargosae* pupfish (KT162099) that encoded deduced amino acid sequences with greater than 86% nucleotide sequence identity and over 85% deduced amino acid sequence identity to predicted *slc12a3*-like transcripts from cyprinodontoids *X. maculatus* (XM_005809179 and XM_005809180) and *P. formosa* (XM_007540339 and XM_007540340).

Results: Identification of Partial cDNAs Encoding Ion Transporters and Aquaporins

Partial-length gene transcripts encoding several ion transporter and aquaporin proteins were isolated and sequenced for the first time from *Cyprinodon nevadensis amargosae* pupfish with degenerate primer PCR followed by Sanger sequencing. These transcripts included an 867-bp nucleotide partial transcript encoding an α_{1a} subunit of NKA (*nka*α_{1a}; GenBank accession no. KT162105), a 1,176-bp nucleotide partial cDNA for *cftr* (KT162091), a 929-bp cDNA encoding *nkcc1* (KT162088), a 1,267-bp transcript encoding *nkcc2* (KT162089), and a 768-bp nucleotide partial cDNA for *nbce1.1* (KT162090). Compared to the multiple isoforms of *slc4a4* identified by Lee and coworkers

(2011) in zebrafish, this partial pupfish *nbce1* cDNA showed highest amino acid sequence identity to the zebrafish zNbce1a isoform (90% identity to *zslc4a4*; accession no. NP_001030156), which is a paralog of the zebrafish zNbce1b cotransporter (81% identity; ABV02975). Examination of the annotated genome for *Cyprinodon variegatus*—a congener to the pupfish *C. nevadensis* of this study—revealed that these two zebrafish *nbc1* isoforms may be paralogs that evolved from a gene duplication event, and separate sets of gene-specific primers were subsequently designed to distinguish between these two pupfish NBCe1 genes.

Separate cDNAs encoding part of the open reading frames of two distinct Na$^+$/H$^+$ exchanger 2 transcripts *nhe2a* (610-bp; KT162092) and *nhe2b* (KT162093), as well as an *nhe3* transcript of 657-bp nucleotides (KT162094), were also amplified and sequenced from *C. n. amargosae*, as were partial cDNAs encoding the 269-bp nucleotides of the open reading frame of vacuolar-type H$^+$-ATPase (*v-ATPase*; KT162095), a 555-bp partial cDNA of the cytosolic isoform of carbonic anhydrase (*ca*; KT162101), a 1,048-bp partial Na$^+$/Cl$^-$ cotransporter transcript (*ncc1*; KT162099), and both *aqp1* (303-bp nucleotides; KT162097) and *aqp3* (386-bp; KT162098). A partial transcript of 421-bp nucleotides encoding the osmosensor transcription factor *tsc22d3* (KT162096) was also amplified and sequenced from *C. n. amargosae*.

Table A1: Degenerate primers used for amplification and sequencing of partial cDNAs from Amargosa pupfish *Cyprinodon nevadensis amargosae*

Transcript, primer	Nucleotide sequence (5′ to 3′)
Na$^+$/K$^+$ ATPase α_{1a} subunit (*nka*α_{1a}):	
ATPaseA1a_for1d	CTG GGC TCC ACC TCC ACC AT
ATPaseA1a_for2d	AC AAC CAG ATC CAY GAA GCY GA
ATPaseA1a_for3d	GAG AAC CAG AGT GGC ACC TC
ATPaseA1a_rev3d	CAC RAT GGC TCC CTG YCT CTG
ATPaseA1a_rev2d	GAG GCA AAG TTR T CRT CCA GCA GG
ATPaseA1a_rev1d	GGG ATG TTA CTG GTC AGR GTG TAG G
Na$^+$/K$^+$/2Cl$^-$ cotransporter-1 (*nkcc1*):	
NKCC1_for1d	CCA RAT GTG AAC TGG GGY TCW TC
NKCC1_for2d	CTT CAG RCC SCA GTG TYT GGT G
NKCC1_for3d	GGT BCA TWC CTT CAC CAA GRA CG
NKCC1_rev3d	GCT GCC TCC ARC TCC ATG TTG TC
NKCC1_rev2d	TCC AGC TCR TTG TCW GTG ATY CTC
NKCC1_rev1d	ATK ACG ATG AGG TTG CTG TG
Na$^+$/K$^+$/2Cl$^-$ cotransporter-2 (*nkcc2*):	
NKCC2_for1d	ATC TCT GGA GAC TTG CGG GAT G
NKCC2_for2d	GTT GTC CGW GAT GCC ACA GG
NKCC2_for3d	GTT GCY TGT GAA CTC GGC TAC GA
NKCC2_rev3d	GAC ACA TCC AGT CCC TGG TTC A
NKCC2_rev2d	GTT GTG AGC ACT TGC TGA GAT GA
NKCC2_rev1d	TCA TCA AAC AGC CAC CAC ACA
Na$^+$/Cl$^-$ cotransporter (*ncc*):	
Ncc_for1d	AAC CTS ACA CCA GAC TGG MGR G
Ncc_for2d	GTA MAA TGG GYT GGA ACT TCA CAG A
Ncc_for3d	TGC TGC CAS YTT RTC YTC TGC
Ncc_rev3d	AAA RTC CAC CAG TGC RGG YCG C

Table A1 (*Continued*)

Transcript, primer	Nucleotide sequence (5′ to 3′)
Ncc_rev2d	AAC GAM CGC ACY TTC CTC TTG TTC
Ncc_rev1d	CAG AGT GTT GGG YTT CAG YTT RC
Na$^+$/HCO$_3^-$ cotransporter-1 (*nbce1*):	
Nbc1_for1d	CAC CAT TTA CAT YGG SGT GCR TGT G
Nbc1_for2d	GCC AGC AAC WSC ATC CTC AAA CC
Nbc1_for3d	GGA CAG GAR ATG GAG TGG AAR GAG
Nbc1_rev3d	CGG TGA AGT CAC TSA CAA AGA AAG G
Nbc1_rev2d	GGT GAT GGC RTT YGT CAC AGT TCC
Nbc1_rev1d	GAA GCT GAT GAG ACA GGM GAA GCC
Cystic fibrosis transmembrane conductance regulator (*cftr*):	
CFTR_for1d	CCT TCY TTT GAY CTG GCA GA CA
CFTR_for2d	GAG AGA CTC GAA AGR GAA TGG GAC
CFTR_for3d	AC CTC AAC AAG CTG GAT GAG AGC
CFTR_rev3d	ACC CTC TGA GGC ACC AAC TC
CFTR_rev2d	TCG TCR TAG GTC AGD CCG AAA AG
CFTR_rev1d	TAG AAG TAG CAG TCT CCR TTR TGC A
Na$^+$/H$^+$ exchanger isoform 2 (*nhe2*):	
NHE2-for1d	CAG GCT CCC TTT GAR ATC GTG C
NHE2-for2d	GCC AAG CTG GGT TTC CAY TGG TC
NHE2-for3d	TGC GTY CTC ATC ATG GTG GGC
NHE2-rev3d	AGG AAG ACR AAG AGS GGR GCG
NHE2-rev2d	GA TGC TRG TGT TGC TGY GCT C
NHE2-rev1d	CGC TRC TCC ACA TCT TCA GRA AGT A
Na$^+$/H$^+$ exchanger isoform 3 (*nhe3*):	
NHE3-for1d	CAT GCC AAA CAA GCT CTT CTT CAS C
NHE3-for2d	TCA TYG GGA CCT GCT GGA AC
NHE3-for3d	CTG TCG CTG TGG GGG TGT CA
NHE3-rev3d	AAC CTT CAT GGC GTA ACG GAC
NHE3-rev2d	AAG ATG ATG GTT CCG AGC CG TTG
NHE3-rev1d	TGA GGA GGA TGA AGC CCG TGT TC
Aquaporin 1 (*aqp1*):	
Aqp1-for1d	CTG GTT GGC ATG ACC CTY TTC AT
Aqp1-for2d	CTC AGC ATC TCM ACA GCT ATY GGG A
Aqp1-for3d	GAC CAG GAR GTG AAG GTG TC
Aqp1-rev2d	GCA ATG ACA CAC AGC ACS AGC
Aqp1-rev1d	TGG GSG ACA GCA GGA AAT CGT A
Aquaporin 3 (*aqp3*):	
Aqp3-for1d	AAC TGK CCC GCT TCT TYC AGA TCC
Aqp3-for2d	TT GGC ACB CTC ATC CTT GTR ATG T
Aqp3-for3d	TCA ACT TTG CCT TYG CCT TYG
Aqp3-rev3d	CCT TGG GGR ATG GGG TTG TTG
Aqp3-rev2d	GAC AAT CCA ATS ACC ARA ACC ACA
Aqp3-rev1d	CGT GGT CCR ADG TCT CTK GC
Carbonic anhydrase 2 (*ca2*):	
CA2_for1d	AAG TAC GAC CCS TCC AMC TGC C
CA2_for2d	CTC AAC AAC GGV CAT CCT TCC AAA G
CA2_for3d	CAA GTG ACC TTC KYG GAC GAC A
CA2_rev3d	GA TTG GYT CYT TGC AGA CDA TCC AGG
CA2_rev2d	GAA GAG GAG GCT GCG GAA KYT G
CA2_rev1d	GGG CGG TAG TTG TTC ACC AT

Table A1 (*Continued*)

Transcript, primer	Nucleotide sequence (5′ to 3′)
Osmotic transcription factor-1 (*ostf1*):	
ostf1-for1d	GTC GCA AWC GTG GCG AGA AG
ostf1-for2d	CAT GAG CAC AGA GAT GTT CGC CA
ostf1-for3d	CTT CTC CAT CTC YTT CTT CTC CTC GC
osft1-rev3d	GGT CRC CYG ACG GYT CTG ATT
osft1-rev2d	GTC CCA TCA ATC ATT TAC AGC MCC G
ostf1-rev1d	C GAA GAG MGA CTA CGA CAA AGA GC
Ribosomal protein L8 (*rpl8*):	
L8_for1d	ACC GCT TCA AGA AGA GGA CMG AG
L8_for2d	CAG TTC ATC TAC TGC GGC RAG AA
L8_rev2d	CCT TCA GGA TGG GYT TGT CAA TAC
L8_rev1d	TGA TGG TTA CCA CCA CCG AAG G
Na$^+$/Cl$^-$ cotransporter-like (*ncc*):[a]	
Ncc-for1d	GGA GCM ACT CTG TCM TCA GCT
Ncc-for2d	GCC TGG TGT CTG CTC CCA ARG
Ncc-for3d	TCA CCA GGT TGG CGT CCR T
Ncc-rev3d	CAG TGA CCA CAT TTC CAC ACA TCA TC
Ncc-rev2d	CCC TGM AGC AGC ATG TTA ACC C
Ncc-rev1d	GCC AGT CTT TCT TGA ARC CCA TSA SC

[a]Gill form. Data for the nongill form are not presented here.

Table A2: Gene-specific primers for SYBR green quantitative polymerase chain reactions in *Cyprinodon nevadensis* pupfish

Transcript	Primer, nucleotide sequence (5′ to 3′)	Amplicon length (bp)	Average efficiency (%)	Accession no. or sequence ID
aqp1	Forward: GCA CAA ATG CTG GGC TCA G	98	98.15	KT162097
	Reverse: GGT GAC ACC GTT AAG AGA GTT TAG			
aqp3	Forward: GCT TGG AAG AGA TAA GTG GAG AA	112	101.26	KT162098
	Reverse: GTG TCC CAC AAG GCA TCA TA			
nbce1.1	Forward: ACG GTC TCC AGT GCA AAT AG	90	100.24	KT162090, JSUU01027575, JSUU01007559, JSUU01014542, JSUU01030693
	Reverse: GTC CTT CTC AGG TTT GTC AGA G			
nbce1.2	Forward: GAG TGG AAC GAT CCT GTT AGA C	107	102.58	JSUU01000712, JSUU01094524
	Reverse: CTC CTT CAG CTC TGC CTT TAG			
cftr	Forward: GGA AAG AGT TCC CTG CTT ATG A	101	99.11	KT162091
	Reverse: CAA GAC GTT TGT GGC GAA TAT G			
ca	Forward: GCT GCC TAG ACT ACT GGA CTT A	97	98.74	KT162101
	Reverse: CTG ACG CTG ATT GGC TCT TT			
nhe2a	Forward: CCT CTT TGT GGG ACT GTT CTT	115	101.90	KT162092
	Reverse: CAG GTA GGA CAG ATA GGA GTA GAG			

1165

Table A2 (*Continued*)

Transcript	Primer, nucleotide sequence (5′ to 3′)	Amplicon length (bp)	Average efficiency (%)	Accession no. or sequence ID
nhe3	Forward: AGT TTC CTT CTT CGT GGT GTC Reverse: GGC TCG ATG ATC TGG ATG TTT	108	103.14	KT162094
nkcc1	Forward: GCC TTC TAC ACT CCT GTG TTT Reverse: GTT CAT CAT GTC TCC GTC TCT C	141	103.18	KT162088
nkcc2	Forward: CCT GGC GTC TTA TGC TCT TAT C Reverse: GTG AGA GCC ACA TGT TGT AGT	104	107.61	KT162089
ncc	Forward: CAG TCC CAG TCC TGT GAA TAT G Reverse: GAC ACC AGC AGT AAT GAG GTA G	90	100.14	KT162099
v-ATPaseβ	Forward: GGT CGA GTA GAG GGA AGA AAT G Reverse: ACC AGT CAG ATC AGG AAT TGG	96	97.33	KT162095
nkaα1a	Forward: CTG GAC GAC GAG TTG AAA GAT G Reverse: GGT CAT CAG GAA GGT GGA AAT G	103	99.71	KT162105
ostf1	Forward: GGA GAA CTA CCT GCT GAA GAA C Reverse: CAC CTG GAC GTT CTG ATT GT	103	97.97	KT162096
ef1α	Forward: CCT GGG TAT TGG ACA AAC TGA Reverse: CGT AGT ACT TGC TGG TCT CAA A	90	101.16	EU906930
rpl8	Forward: GAC CAA GAA GTC CAG AGT CAA G Reverse: TCA GGA TGG GCT TGT CAA TAC	116	99.42	KJ719257

Table A3: GenBank accession or Ensembl numbers for amino acid sequences used in phylogenetic analysis of NBCe1

Protein name, species common name	Species scientific name	GenBank accession or Ensembl no.
NBCe1:		
Human	*Homo sapiens*	AF053754
Rat	*Rattus norvegicus*	AAC40034
Tropical clawed frog	*Xenopus tropicalis*	XP_002940622
Green anole	*Anolis carolinensis*	XM_008112171
Green sea turtle	*Chelonia mydas*	XM_007065905
American alligator	*Alligator mississippiensis*	XM_014607383
Chicken	*Gallus gallus*	XP_015131894
Medium-ground finch	*Geospiza fortis*	XP_014165850
Burmese python	*Python bivittatus*	XM_007437122
Tiger salamander	*Ambystoma tigrinum*	AAB61339

Table A3 (*Continued*)

Protein name, species common name	Species scientific name	GenBank accession or Ensembl no.
NBCe1-like:		
Coelacanth	*Latimeria chalumnae*	XP_014353039
NBCe1.1:		
Threespine stickleback	*Gasterosteus aculeatus*	ENSGACG00000014471
Mummichog	*Fundulus heteroclitus*	GQ376030
Green-spotted pufferfish	*Tetraodon nigroviridi*	CAG07774
Atlantic cod	*Gadus morhua*	ENSGMOG00000014112
Sheepshead minnow	*Cyprinodon variegatus*	XM_015403828
Zebrafish	*Danio rerio*	NM_001034984
Nile tilapia	*Oreochromis niloticus*	XP_003444524
Rainbow trout	*Oncorhynchus mykiss*	XP_021460748
Coho salmon	*Oncorhynchus kisutch*	XP_020332471
Atlantic salmon	*Salmo salar*	NC_027323
NBCe1.2:		
Threespine stickleback	*G. aculeatus*	ENSGACG00000015864
Mefugu	*Takifugu obscurus*	AB362567
Japanese dace	*Tribolodon hakonensis*	BAB83084
Mummichog	*F. heteroclitus*	XM_012853007
Green-spotted pufferfish	*T. nigroviridi*	CAF97103
Atlantic cod	*G. morhua*	ENSGMOG00000008121
Sheepshead minnow	*C. variegatus*	XM_015388382
Zebrafish	*D. rerio*	EF634453
Nile tilapia	*O. niloticus*	XP_003449699
NBCe1.2a:		
Rainbow trout	*O. mykiss*	XP_021446201, XP_020321135
Coho salmon	*O. kisutch*	XP_020314165
Atlantic salmon	*S. salar*	XP_013996420
NBCe1.2b:		
Rainbow trout	*O. mykiss*	AF434166
Coho salmon	*O. kisutch*	XP_020321135
Atlantic salmon	*S. salar*	XP_013983531

Literature Cited

Atkinson M.J. and C. Bingman. 1997. Elemental composition of commercial seasalts. J Aquaricult Aquat Sci 8:39–43.

Barlow G.W. 1958. Daily movements of desert pupfish, *Cyprinodon macularius*, in shore pools of the Salton Sea, California. Ecology 39:580–587.

Berdan E.L. and R.C. Fuller. 2012. Interspecific divergence of ionoregulatory physiology in killifish: insight into adaptation and speciation. J Zool (Lond) 287:283–291.

Blondeau-Bidet E., M. Bossus, G. Maugars, E. Farcy, J.-H. Lignot, and C. Lorin-Nebel. 2016. Molecular characterization and expression of Na$^+$/K$^+$-ATPase α1 isoforms in the European sea bass *Dicentrarchus labrax* osmoregulatory tissues following salinity transfer. Fish Physiol Biochem 42:1647–1664.

Bodinier C., V. Boulo, C. Lorin-Nebel, and G. Charmantier. 2009. Influence of salinity on the localization and expression of the CFTR chloride channel in the ionocytes of *Dicentrarchus labrax* during ontogeny. J Anat 214:318–329.

Breves J.P., S. Hasegawa, M. Yoshioka, B.K. Fox, L.K. Davis, D.T. Lerner, Y. Takei, T. Hirano, and E.G. Grau. 2010. Acute salinity challenges in Mozambique and Nile tilapia: differential responses of plasma prolactin, growth hormone and branchial expression of ion transporters. Gen Comp Endocrinol 167:135–142.

Breves J.P., M. Inokuchi, Y. Tamaguchi, A.P. Seale, B.L. Hunt, S. Watanabe, D.T. Lerner, T. Kaneko, and E.G. Grau. 2016. Hormonal regulation of aquaporin 3: opposing actions of prolactin and cortisol in tilapia gill. J Endocrinol 230:325–337.

Brix K.V. and M. Grosell. 2012. Comparative characterization of Na$^+$ transport in *Cyprinodon variegatus variegatus* and *Cyprinodon variegatus hubbsi*: a model species complex for studying teleost invasion of freshwater. J Exp Biol 215:1199–1209.

———. 2013. Characterization of Na$^+$ uptake in the endangered desert pupfish, *Cyprinodon macularius* (Baird and Girard). Conserv Physiol 1:cot005. doi:10.1093/conphys/cot005.

Brunelli E., A. Mauceri, F. Salvatore, A. Giannetto, M. Maisano, and S. Tripepi. 2010. Localization of aquaporin 1 and 3 in the gills of the rainbow wrasse *Coris julis*. Acta Histochem 112:251–258.

Chang M.-H., C. Plata, Y. Kurita, A. Kato, S. Hirose, and M.F. Romero. 2012. Euryhaline pufferfish NBCe1 differs from nonmarine species NBCe1 physiology. Am J Physiol Cell Physiol 302:C1083–C1095.

Choi C.Y. and K.W. An. 2008. Cloning and expression of Na$^+$/K$^+$-ATPase and osmotic stress transcription factor 1 mRNA in black porgy, *Acanthopagrus schlegeli* during osmotic stress. Comp Biochem Physiol B 149:91–100.

Chow S.C. and C.K.C. Wong. 2011. Regulatory function of hyperosmotic stress-induced signaling cascades in the expression of transcriptional factors and osmolyte transporters in freshwater Japanese eel primary gill cell culture. J Exp Biol 214:1264–1270.

Cutler C.P. and G. Cramb. 2002. Two isoforms of the Na$^+$/K$^+$/2Cl$^-$ cotransporter are expressed in the European eel (*Anguilla anguilla*). Biochim Biophys Acta 1566:92–103.

Cutler C.P., A.-S. Martinez, and G. Cramb. 2007. The role of aquaporin 3 in teleost fish. Comp Biochem Physiol A 148:82–91.

Edwards S.L. and W.S. Marshall. 2013. Principles and patterns of osmoregulation and euryhaline in fishes. Pp. 1–44 in S.D. McCormick, A.P. Farrell, and C.J. Brauner, eds. Euryhaline fishes. Academic Press, Oxford.

Edwards S.L., B. Wall, A. Morrison-Shetlar, S. Sligh, J. Weakley, and J. Claiborne. 2005. The effect of environmental hypercapnia and salinity on the expression of NHE-like isoforms in the fills of a euryhaline fish (*Fundulus heteroclitus*). J Exp Zool A 303:464–475.

Epstein F.H., A.I. Katz, and G.E. Pickford. 1967. Sodium- and potassium-activated adenosine triphosphatase of gills: role in adaptation of teleosts to salt water. Science 156:1245–1247.

Evans D.H., P.M. Piermarini, and K.P. Choe. 2005. The multifunctional fish gill: dominant site of gas exchange, osmoregulation, acid-base regulation, and excretion of nitrogenous waste. Physiol Rev 85:97–177.

Fiol D.F., S.Y. Chan, and D. Kültz. 2006. Regulation of osmotic stress transcription factor 1 (Ostf1) in tilapia (*Oreochromis mossambicus*) gill epithelium during salinity stress. J Exp Biol 209:3257–3265.

Fiol D.F. and D. Kültz. 2005. Rapid hyperosmotic coinduction of two tilapia (*Oreochromis mossambicus*) transcription factors in gill cells. Proc Natl Acad Sci USA 102:927–932.

———. 2007. Osmotic stress sensing and signaling in fishes. FEBS J 274:5790–5798.

Flemmer A.W., M.Y. Monette, M. Djurisic, B. Dowd, R.B. Darman, I. Gimenez, and B. Forbush. 2010. Phosphorylation state of the Na$^+$K$^+$2Cl$^-$ cotransporter (NKCC) in the gills of

Atlantic killifish (*Fundulus heteroclitus*) during acclimation to water of varying salinity. J Exp Biol 213:1558–1566.

Garty H., and S.J.D. Karlish. 2006. Role of FXYD proteins in ion transport. Annu Rev Physiol 68:431–459.

Gerking S.D. and R.M. Lee. 1980. Reproductive performance of the desert pupfish (*Cyprinodon n. nevadensis*) in relation to salinity. Environ Biol Fish 5:375–378.

Ghedotti M.J. and M.P. Davis. 2013. Phylogeny, classification, and evolution of salinity tolerance of the North American topminnows and killifishes, family Fundulidae (Teleostei: Cyprinodontiformes). Fieldiana Life Earth Sci 7:1–65.

Giffard-Mena I., V. Boulo, F. Aujoulat, H. Fowden, R. Castille, G. Charmantier, and G. Cramb. 2007. Aquaporin molecular characterization in the sea-bass (*Dicentrarchus labrax*): the effect of salinity on AQP1 and AQP3 expression. Comp Biochem Physiol A 148:430–444.

Gilmore R.G., D.W. Cooke, and C.J. Donohue. 1982. A comparison of the fish populations and habitat in open and closed salt marsh impoundments in east-central Florida. Northeast Gulf Sci 5:25–37.

Goss G.G. and C.M. Wood. 1990. Na$^+$ and Cl$^-$ uptake kinetics, diffusive effluxes and acidic equivalent fluxes across the gills of rainbow trout. II. Responses to bicarbonate infusion. J Exp Biol 152:549–571.

Gross E., A. Pushkin, N. Abuladze, O. Fedotoff, and I. Kurtz. 2002. Regulation of the sodium bicarbonate cotransporter kNBC1 function: role of Asp^{986}, Asp^{988} and kNBC1-carbonic anhydrase II binding. J Physiol 544:679–685.

Hiroi J. and S.D. McCormick. 2012. New insights into gill ionocyte and ion transporter function in euryhaline and diadromous fish. Respir Physiol Neurobiol 184:257–268.

Hiroi J., S. Yasumasu, S.D. McCormick, P.-P. Hwang, and T. Kaneko. 2008. Evidence for an apical Na-Cl cotransporter involved in ion uptake in a teleost fish. J Exp Biol 211:2584–2599.

Hsu H.-H., L.-Y. Lin, Y.-C. Tseng, J.-L. Horng, and P.-P. Hwang. 2014. A new model for fish ion regulation: identification of ionocytes in freshwater- and seawater-acclimated medaka (*Oryzias latipes*). Cell Tiss Res 357:225–243.

Hwang P.-P., T.-H. Lee, and L.-Y. Lin. 2011. Ion regulation in fish gills: recent progress in the cellular and molecular mechanisms. Am J Physiol Regul Integr Comp Physiol 301:R28–R47.

Inokuchi M., J. Hiroi, S. Watanabe, K.M. Lee, and T. Kaneko. 2008. Gene expression and morphological localization of NHE3, NCC, and NKCC1a in branchial mitochondria-rich cells of Mozambique tilapia (*Oreochromis mossambicus*) acclimated to a wide range of salinities. Comp Biochem Physiol A 151:151–158.

Ivanis G., A.J. Esbaugh, and S.F. Perry. 2008. Branchial expression and localization of SLC9A2 and SLC9A3 sodium/hydrogen exchangers and their possible role in acid-base regulation in freshwater rainbow trout (*Oncorhynchus mykiss*). J Exp Biol 211:2467–2477.

Jensen M.K., S.S. Madsen, and K. Kristiansen. 1998. Osmoregulation and salinity effects on the expression and activity

of Na$^+$,K$^+$-ATPase in the gills of European sea bass, *Dicentrarchus labrax* (L.). J Exp Zool 282:290–300.

Jordan F., D.C. Haney, and F.G. Nordlie. 1993. Plasma osmotic regulation and routine metabolism in the Eustis pupfish, *Cyprinodon variegatus hubbsi* (Teleostei: Cyprinodontidae). Copeia 1993:784–789.

Jorgensen P.L., K.O. Håkansson, and S.J.D. Karlish. 2003. Structure and mechanism of Na,K-ATPase: functional sites and their interactions. Annu Rev Physiol 65:817–849.

Jung D., J.D. Sato, J.R. Shaw, and B.A. Stanton. 2012. Expression of aquaporin 3 in gills of the Atlantic killifish (*Fundulus heteroclitus*): effects of seawater acclimation. Comp Biochem Physiol A 161:320–326.

Kang C.K., H.J. Tsai, C.C. Liu, T.H. Lee, and P.P. Hwang. 2010. Salinity-dependent expression of a Na$^+$, K$^+$, 2Cl$^-$ cotransporter in gills of the brackish medaka *Oryzias dancena*: a molecular correlation for hypoosmoregulatory endurance. Comp Biochem Physiol A 157:7–18.

Karnaky K.J., Jr., S.A. Ernst, and C.W. Philpott. 1976. Teleost chloride cell. I. Response of pupfish *Cyprinodon variegatus* gill Na,K-ATPase and chloride cell fine structure to various high salinity environments. J Cell Biol 70:144–156.

Katoh F., S. Hyodo, and T. Kaneko. 2003. Vacuolar-type proton pump in the basolateral plasma membrane energizes ion uptake in branchial mitochondria-rich cells of killifish *Fundulus heteroclitus*, adapted to a low ion environment. J Exp Biol 206:793–803.

Katoh F. and T. Kaneko. 2003. Short-term transformation and long-term replacement of branchial chloride cells in killifish transferred from seawater to freshwater, revealed by morphofunctional observations and a newly established "time-differential double fluorescent staining" technique. J Exp Biol 206:4113–4123.

Kolarevic J., H. Takle, O. Felip, E. Ytteborg, R. Selset, C.M. Good, G. Baeverfjord, T. Asgard, and B.F. Terjesen. 2012. Molecular and physiological responses to long-term sublethal ammonia exposure in Atlantic salmon (*Salmo salar*). Aquat Toxicol 124–125:48–57.

Kültz D. 2005. Rapid hyperosmotic coinduction of two tilapia (*Oreochromis mossambicus*) transcription factors in gill cells. Proc Natl Acad Sci USA 102:927–932.

———. 2013. Osmosensing. Pp. 45–68 in S.D. McCormick, A.P. Farrell, and C.J. Brauner, eds. Euryhaline fishes. Academic Press, Oxford.

Kumar S., G. Stecher, and K. Tamura. 2016. MEGA7: molecular evolutionary genetics analysis version 7.0 for bigger datasets. Mol Biol Evol 33:1870–1874.

Kurita Y., T. Nakada, A. Kato, H. Doi, A.C. Mistry, M.-H. Chang, M.F. Romero, and S. Hirose. 2008. Identification of intestinal bicarbonate transporters involved in formation of carbonate precipitates to stimulate water absorption in marine teleost fish. Am J Physiol Regul Integr Comp Physiol 294:R1402–R1412.

LaBounty J.F. and J.E. Deacon. 1972. *Cyprinodon milleri*, a new species of pupfish (family Cyprinodontidae) from Death Valley, California. Copeia 1972:769–780.

Larkin M.A., G. Blackshields, N.P. Brown, R. Chenna, P.A. McGettigan, H. McWilliam, F. Valentin, et al. 2007. Clustal W and Clustal X version 2.0. Bioinformatics 23:2947–2948.

Laverty G. and E. Skadhauge. 2012. Adaptation of teleosts to very high salinity. Comp Biochem Physiol A 163:1–6.

Lee Y.C., J.J. Yan, S.A. Cruz, J.L. Horng, and P.P. Hwang. 2011. Anion exchanger 1b, but not sodium-bicarbonate cotransporter 1b, plays a role in transport functions of zebrafish H$^+$-ATPase-rich cells. Am J Physiol Cell Physiol 300:C295–C307.

Lema S.C. 2010. Identification of multiple vasotocin receptor cDNAs in teleost fish: sequences, phylogenetic analysis, sites of expression, and regulation in the hypothalamus and gill in response to hyperosmotic challenge. Mol Cell Endocrinol 321:215–230.

Lema S.C., K.E. Sanders, and K.A. Walti. 2015. Arginine vasotocin, isotocin and nonapeptide receptor gene expression link to social status and aggression in sex-dependent patterns. J Neuroendocriol 27:142–157.

Li Z., E.Y. Lui, J.M. Wilson, Y.K. Ip, Q. Lin, T.J. Lam, and S.H. Lam. 2014. Expression of key ion transporters in the gill and esophageal-gastrointestinal tract of euryhaline Mozambique tilapia *Oreochromis mossambicus* acclimated to fresh water, seawater and hypersaline water. PLoS ONE 9:e87591. doi:10.1371/journal.pone.0087591.

Lignot J.-H., C.P. Cutler, N. Hazon, and G. Cramb. 2002. Immunolocalisation of aquaporin 3 in the gill and the gastrointestinal tract of the European eel *Anguilla anguilla* (L.). J Exp Biol 205:2653–2663.

Lin H., S.C. Pfeiffer, A.W. Vogl, J. Pan, and D.J. Randall. 1994. Immunolocalization of H$^+$-ATPase in the gill epithelia of rainbow trout. J Exp Biol 195:169–183.

Lin T.Y., B.K. Liao, J.L. Horng, J.J. Yan, C.D. Hsiao, and P.P. Hwang. 2008. Carbonic anhydrase 2-like a and 15a are involved in acid-base regulation and Na$^+$ uptake in zebrafish H$^+$-ATPase-rich cells. Am J Physiol Cell Physiol 294:C1250–C1260.

MacIver B., C.P. Cutler, J. Yin, M.G. Hill, M.L. Zeidel, and W.G. Hill. 2009. Expression and functional characterization of four aquaporin water channels from the European eel (*Anguilla anguilla*). J Exp Biol 212:2856–2863.

Madsen S.S., M.B. Engelund, and C.P. Cutler. 2015. Water transport and functional dynamic of aquaporins in osmoregulatory organs of fishes. Biol Bull 229:70–92.

Mancera J.M. and S.D. McCormick. 2000. Rapid activation of gill Na$^+$,K$^+$-ATPase in the euryhaline teleost *Fundulus heteroclitus*. J Exp Biol 287:263–274.

Marshall W.S., S.E. Bryson, P. Darling, C. Whitten, M. Patrick, M. Wilkie, C.M. Wood, and N.J. Buckland. 1997. NaCl transport and ultrastructure of opercular epithelium from a freshwater-adapted euryhaline teleost, *Fundulus heteroclitus*. J Exp Biol 277:23–37.

Marshall W.S., T.R. Emberley, T.D. Singer, D.E. Bryson, and S.D. McCormick. 1999. Time course of salinity adaptation in a strongly euryhaline estuarine teleost, *Fundulus heteroclitus*: a multivariate approach. J Exp Biol 202:1535–1544.

Marshall W.S., E.A. Lynch, and R.R.F. Cozzi. 2002. Redistribution of immunofluorescence of CFTR anion channel and NKCC cotransporter in chloride cells during adaptation of the killifish *Fundulus heteroclitus* to sea water. J Exp Biol 205:1265–1273.

McCormick S.D. 1993. Methods for non-lethal gill biopsy and measurement of Na$^+$, K$^+$-ATPase activity. Can J Fish Aquat Sci 50:656–658.

McCormick S.D., A.M. Regish, and A.K. Christensen. 2009. Distinct freshwater and seawater isoforms of Na$^+$/K$^+$-ATPase in gill chloride cells of Atlantic salmon. J Exp Biol 212:3994–4001.

Miller R.R. 1950. Speciation in fishes of the genera *Cyprinodon* and *Empetrichthys*, inhabiting the Death Valley region. Evolution 4:155–163.

Mistry A.C., S. Honda, Y. Hirata, A. Kato, and S. Hirose. 2001. Eel urea transporter is localized to chloride cells and is salinity dependent. Am J Physiol Regul Integr Comp Physiol 281:R1594–R1604.

Moorman B.P., M. Inokuchi, Y. Yamaguchi, D.T. Lerner, E.G. Grau, and A.P. Seale. 2014. The osmoregulatory effects of rearing Mozambique tilapia in a tidally changing salinity. Gen Comp Endocrinol 207:94–102.

Moorman B.P., D.T. Lerner, E.G. Grau, and A.P. Seale. 2015. The effects of acute salinity challenges on osmoregulation in Mozambique tilapia reared in a tidally changing salinity. J Exp Biol 218:731–739.

Naiman R.J., S.D. Gerking, and R.E. Stuart. 1976. Osmoregulation in the Death Valley pupfish *Cyprinodon milleri* (Pisces: Cyprinodontidae). Copeia 1976:807–810.

Nilsen T.P., L.O.E. Ebbesson, S.S. Madsen, S.D. McCormick, E. Andersson, B.T. Björnsson, P. Prunet, and S.O. Stefansson. 2007. Differential expression of gill Na$^+$,K$^+$-ATPase α- and β-subunits, Na$^+$,K$^+$,2Cl$^-$ cotransporter and CFTR anion channel in juvenile anadromous and landlocked Atlantic salmon *Salmo salar*. J Exp Biol 210:2885–2896.

Nordlie F.G. 1985. Osmotic regulation in the sheepshead minnow *Cyprinodon variegatus* Lacépède. J Fish Biol 26:161–170.
———. 2006. Physicochemical environments and tolerances of cyprinodontoid fishes found in estuaries and salt marshes of eastern North America. Rev Fish Biol Fish 16:51–106.

Parks S.K., M. Tresguerres, and G.G. Goss. 2007. Interactions between Na$^+$ channels and Na$^+$-HCO$_3^-$ cotransporters in the freshwater fish gill MR cell: a model for transepithelial Na$^+$ uptake. Am J Physiol Cell Physiol 292:C935–C944.

Patrick M.L., P. Pärt, W.S. Marshall, and C.M. Wood. 1997. Characterization of ion and acid-base transport in the fresh water adapted mummichog (*Fundulus heteroclitus*). J Exp Zool 279:208–219.

Patrick M.L. and C.M. Wood. 1999. Ion and acid-base regulation in the freshwater mummichog (*Fundulus heteroclitus*): a departure from the standard model for freshwater teleosts. Comp Biochem Physiol A 122:445–456.

Perry S.F., A. Shahsavarani, T. Georgalis, M. Bayaa, M. Furimsky, and S.L.Y. Thomas. 2003. Channels, pumps, and exchangers in the gill and kidney of freshwater fishes: their role in ionic and acid-base regulation. J Exp Zool 300:53–62.

Prodocimo V., F. Galvez, C.A. Freire, and C.M. Wood. 2007. Unidirectional Na$^+$ and Ca^{2+} fluxes in two euryhaline teleost fishes, *Fundulus heteroclitus* and *Oncorhynchus mykiss*, acutely submitted to a progressive salinity increase. J Comp Physiol B 177:519–528.

Renfro J.L. and L.G. Hill. 1971. Osmotic acclimation of the Red River pupfish, *Cyprinodon rubrofluviatilis*. Comp Biochem Physiol 40:711–714.

Richards J.G., J.W. Semple, J.S. Bystriansky, and P.M. Schulte. 2003. Na$^+$/K$^+$-ATPase α-isoform switching in gills of rainbow trout (*Oncorhynchus mykiss*) during salinity transfer. J Exp Biol 206:4475–4486.

Romero M.F., A.-P. Chen, M.D. Parker, and W.F. Boron. 2013. The SLC4 family of bicarbonate (HCO$_3^-$) transporters. Mol Aspects Med 34:159–182.

Romero M.F., C.M. Fulton, and W.F. Boron. 2004. The SLC4 family of HCO$_3^-$ transporters. Pfluegers Arch 447:495–509.

Sardella B., V. Matey, J. Cooper, R. Gonzalez, and C.J. Brauner. 2004. Physiological, biochemical, and morphological indicators of osmoregulatory stress in 'California' Mozambique tilapia (*Oreochromis mossambicus* × *O. urolepis hornorum*) exposed to hypersaline water. J Exp Biol 207:1399–1413.

Schultz E.T. and S.D. McCormick. 2013. Euryhalinity in an evolutionary context. Pp. 477–533 in S.D. McCormick, A.P. Farrell, and C.J. Brauner, eds. Euryhaline fishes. Academic Press, Oxford.

Scott G.R., D.W. Baker, P.M. Schulte, and C.M. Wood. 2008. Physiological and molecular mechanisms of osmoregulatory plasticity in killifish after seawater transfer. J Exp Biol 211:2450–2459.

Scott G.R., J.B. Claiborne, S.L. Edwards, P.M. Schulte, and C.M. Wood. 2005. Gene expression after freshwater transfer in gills and opercular epithelia of killifish: insight into divergent mechanisms of ion transport. J Exp Biol 208:2719–2729.

Scott G.R., J.G. Richards, B. Forbush, P. Isenring, and P.M. Schulte. 2004. Changes in gene expression in gills of the euryhaline killifish *Fundulus heteroclitus* after abrupt salinity transfer. Am J Physiol Cell Physiol 287:C300–309.

Scott G.R. and P.M. Schulte. 2005. Intraspecific variation in gene expression after seawater transfer in gills of the euryhaline killifish *Fundulus heteroclitus*. Comp Biochem Physiol A 141:176–182.

Seo M.Y., M. Mekuchi, K. Teranishi, and T. Kaneko. 2013. Expression of ion transporters in gill mitochondrion-rich cells in Japanese eel acclimated to a wide range of environmental salinity. Comp Biochem Physiol A 166:323–332.

Shaw J.R., J.D. Sato, J. VanderHeide, T. LaCasse, C.E. Stanton, A. Lankowski, S.E. Stanton, et al. 2008. The role of SGK and CFTR in acute adaptation to seawater in *Fundulus heteroclitus*. Cell Physiol Biochem 22:69–78.

Simpson D.G. and G. Gunter. 1956. Notes on habitats, systematic characteristics and life histories of Texas salt-water cyprinodontes. Tulane Stud Zool 4:115–134.

Singer T.D., S.J. Tucker, W.S. Marshall, and C.F. Higgins. 1998. A divergent CFTR homologue: highly regulated salt trans-

port in the euryhaline teleost *F. heteroclitus*. Am J Physiol Cell Physiol 274:C715–C723.

Soltz D.L. and R.J. Naiman. 1978. The natural history of native fishes in the Death Valley system. Science Series, no. 30. Los Angeles: Natural History Museum of Los Angeles County.

Stuenkel E.L. and S.D. Hillyard. 1980. Effects of temperature and salinity on gill Na$^+$-K$^+$ ATPase activity in the pupfish, *Cyprinodon salinus*. Comp Biochem Physiol A 67:179–182.

———. 1981. The effects of temperature and salinity acclimation on metabolic rate and osmoregulation in the pupfish *Cyprinodon salinus*. Copeia 1981:411–417.

Sullivan G.V., J.N. Fryer, and S.F. Perry. 1995. Immunolocalization of proton pumps (H$^+$ ATPase) in pavement cells of rainbow trout gill. J Exp Biol 198:2619–2629.

———. 1996. Localization of mRNA for the proton pump (H$^+$ ATPase) and Cl$^-$/HCO$_3^-$ exchanger in the rainbow trout gill. Can J Zool 74:2095–2103.

Tanko D.J. and P.A. Glancy. 2001. Flooding in the Amargosa River drainage basin, February 23–24, 1998, southern Nevada and eastern California, including the Nevada test site. US Geol Surv Fact Sheet 036–01. https://pubs.usgs.gov/fs/fs-036-01/book/fs03601.pdf.

Tingaud-Sequeira A., M. Calusinska, R.N. Finn, F. Chauvigné, J. Lozano, and J. Cerdà. 2010. The zebrafish genome encodes the largest vertebrate repertoire of functional aquaporins with dual paralogy and substrate specificities similar to mammals. BMC Evol Biol 10:38. doi:10.1186/1471-2148-10-38.

Tipsmark C.K., J.P. Breves, A.P. Seale, D.T. Lerner, T. Hirano, and E.G. Grau. 2011. Switching of Na$^+$,K$^+$-ATPase isoforms by salinity and prolactin in the gill of a cichlid fish. J Endocrinol 209:237–244.

Tipsmark C.K., K.J. Sorensen, and S.S. Madsen. 2010. Aquaporin expression dynamics in osmoregulatory tissues of Atlantic salmon during smoltification and seawater acclimation. J Exp Biol 213:368–379.

Towle D.W., M.E. Gilman, and J.D. Hempel. 1977. Rapid modulation of gill Na$^+$+K$^+$-dependent ATPase activity during acclimation of the killifish *Fundulus heteroclitus* to salinity change. J Exp Zool 202:179–186.

Tse W.K.F. 2014. The role of osmotic stress transcription factor 1 in fishes. Front Zool 11:86. doi:10.1186/s12983-014-0086-5.

Tse W.K.F., D.W.T. Au, and C.K.C. Wong. 2006. Characterization of ion channel and transporter mRNA expression in isolated gill chloride and pavement cells of seawater acclimating eels. Biochem Biophys Res Commun 346:1181–1190.

Tse W.K.F., S.C. Chow, and C.K.C. Wong. 2012. Eel osmotic stress transcription factor 1 (Ostf1) is highly expressed in gill mitochondria-rich cells, where ERK phosphorylated. Front Zool 9:3. doi:10.1186/1742-9994-9-3.

Tse W.K.F., K.P. Lai, and Y. Takei. 2011. Medaka osmotic stress transcription factor 1b (Ostf1b/TSC22D3-2) triggers hyperosmotic responses of different ion transporters in medaka gill and human embryonic kidney cells via the JNK signalling pathway. Int J Biochem Cell B 43:1764–1775.

Velotta J.P., J.L. Wegrzyn, S. Ginzburg, L. Kang, S. Czesny, R.J. O'Neill, S.D. McCormick, P. Michalak, and E.T. Schultz. 2017. Transcriptomic imprints of adaptation to fresh water: parallel evolution of osmoregulatory gene expression in the alewife. Mol Ecol 26:831–848.

Wang Y.-F., Y.-C. Tseng, J.-J. Yan, J. Hiroi, and P.-P. Hwang. 2009. Role of SLC12A10.2, a Na-Cl cotransporter-like protein, in a Cl uptake mechanism in zebrafish (*Danio rerio*). Am J Physiol Regul Integr Comp Physiol 296:R1650–R1660.

Watanabe S., T. Kaneko, and K. Aida. 2005. Aquaporin-3 expressed in the basolateral membrane of gill chloride cells in Mozambique tilapia *Oreochromis mossambicus* adapted to freshwater and seawater. J Exp Biol 208:2673–2682.

Whitehead A. 2010. The evolutionary radiation of diverse osmotolerant physiologies in killifish (*Fundulus* sp.). Evolution 64:2070–2085.

Whitehead A., F. Galvez, S. Zhang, L.M. Williams, and M.F. Oleksiak. 2010. Functional genomics of physiological plasticity and local adaptation in killifish. J Heredity 102:499–511.

Wood C.M. and M. Grosell. 2008. A critical analysis of transepithelial potential in intact killifish (*Fundulus heteroclitus*) subjected to acute and chronic changes in salinity. J Comp Physiol B 178:713–727.

Wood C.M. and P. Laurent. 2003. Na$^+$ versus Cl$^-$ transport in the intact killifish after rapid salinity transfer. Biochim Biophys Acta Biomembranes 1618:106–119.

Yan J.J., M.Y. Chou, T. Kaneko, and P.P. Hwang. 2007. Gene expression of Na$^+$/H$^+$ exchanger in zebrafish H$^+$-ATPase-rich cells during acclimation to low-Na$^+$ and acidic environments. Am J Physiol Cell Physiol 293:C1814–C1823.